Elements of Photonics, Volume I: In Free Space and Special Media. Keigo Iizuka

ISBNs: 0-471-83938-8 (Hardback); 0-471-22107-4 (Electronic)

8

PHASE CONJUGATE OPTICS

This chapter deals with optical phase conjugation that can be generated in a medium with third order nonlinear susceptibility. The path of the phase conjugate wave retraces itself. This is analogous to playing a videotape backward, or in other words, a time-reversed videotape. The chapter begins with an illustration of the striking differences between an ordinary mirror and a phase conjugate mirror.

8.1 THE PHASE CONJUGATE MIRROR

The manner of reflection from a phase conjugate mirror is compared with that of a plain, ordinary mirror in Fig. 8.1 [1]. With the ordinary mirror in Fig. 8.1a, the reflected wave not only changes its direction in accordance with the orientation of the mirror, but also keeps on diverging if the incident light is diverging. On the other hand, the wave reflected from the phase conjugate mirror heads back to where it came from regardless of the orientation of the mirror. Furthermore, if the incident wave is a diverging wave, the reflected wave becomes a converging wave. The wave reflected from the phase conjugate mirror is called a phase conjugate wave.

The phase conjugate wave formed by an ordinary hologram provides greater insight into this phenomenon, as explained in the next section.

8.2 GENERATION OF A PHASE CONJUGATE WAVE USING A HOLOGRAM

A phase conjugate wave can be generated almost in real time if a special type of nonlinear crystal or gas is used. Even though an ordinary hologram cannot operate in real time, it is useful for explaining the principle of generating the phase conjugate wave [2,3]. Figure 8.2 shows the geometry for recording a hologram using photographic film. Let O be the field emanating from a point object o onto the photographic film, and R be the reference wave emanating from the reference point source r onto

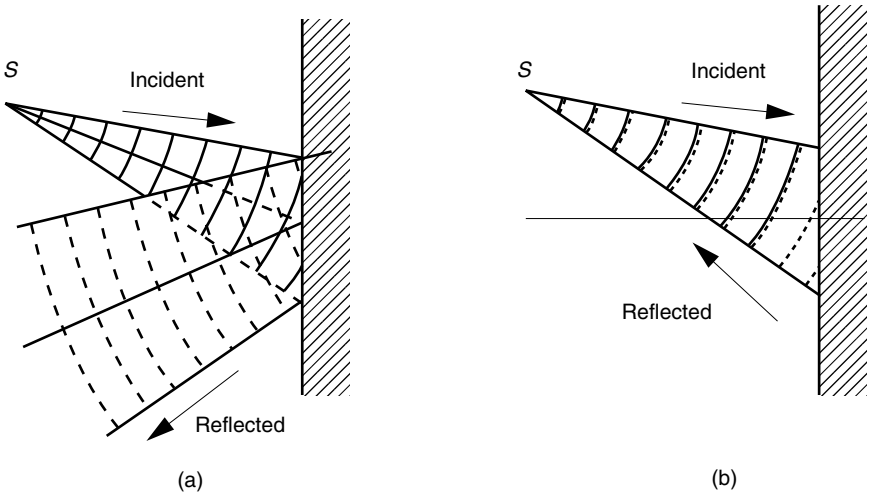

Figure 8.1 Difference between (a) a plain, ordinary mirror and (b) a phase conjugate mirror.

the same photographic film. The O and R waves form an interference fringe pattern. The exposed and developed photographic film is filled with hyperbolic-shaped, silver-grained, miniature mirrors as shown in Fig. 8.2. The transmittance of such a fringe pattern was given in Eq. (1.261) as

$$t = t_0 - \beta[|R|^2 + |O|^2 + OR^* + O^*R] \tag{8.1}$$

When this hologram is illuminated by R^*, the fourth term, βO^*R, in the square bracket generates the phase conjugate wave $|R|^2O^*$. This is the shortest mathematical explanation of the generation of the phase conjugate wave O^*. Here, however, a graphical explanation is attempted because it can readily be used for explaining related phenomena.

Referring back to Fig. 8.2, a new point light source r' and a convex lens are arranged such that its path retraces the original reference wave R from the opposite direction. This light is R^*, the complex conjugate of the original R (we see in Section 1.5.4 that Eq. (1.162) is the complex conjugate of Eq. (1.161).), and the hologram is illuminated by R^*. The normals to the miniature mirrors are always oriented in the plane of the bisector of the angle between the object O and reference R beams. For instance, the surface of the small mirror at point c is in a plane that bisects $\angle ocr$ made by $\overline{oc}$ and $\overline{cr}$, and thus, $\alpha = \alpha'$ and R^* is reflected toward the object point o.

In conclusion, R^* (pump wave) from r' generates a wave that traces back the object wave O and converges to the source point. This wave is O^*, the phase conjugate of the O wave. The phase conjugate wave can be separated from the signal wave by means of a half-mirror (HM). It would seem that the O^* wave is the exact retrace of the O wave but the photons of the O^* wave come from the pump wave R^*, and *not from the original point source o*. The intensity of the reflected wave is controlled by the efficiency of the small mirrors and the intensity of the pump wave R^*. The intensity of the phase conjugate wave O^* can be even larger than that of the O wave and, as such, serves as a useful way of amplifying the intensity.

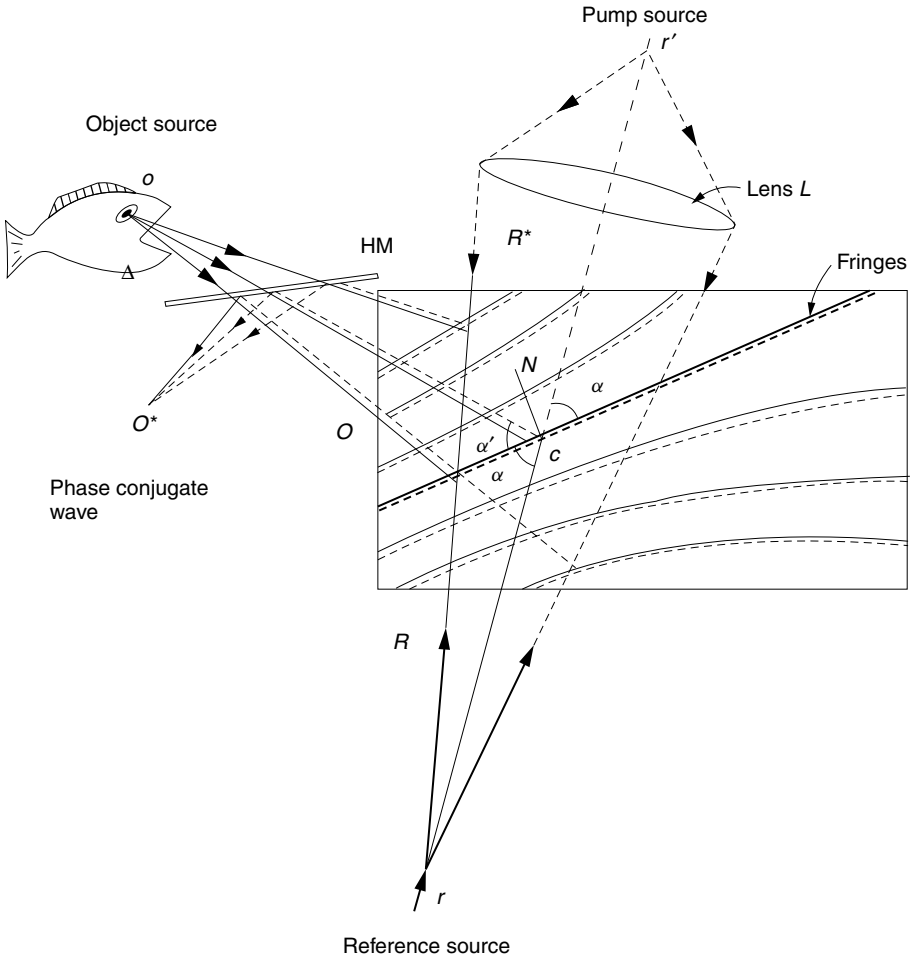

Figure 8.2 Phase conjugate wave generated by a hologram. HM is a half-mirror.

In the hologram in Fig. 8.2, the generation of the phase conjugate wave requires the participation of the following three waves: the object wave O, the reference wave R, and the reconstruction wave R^*. Including the phase conjugate wave O^*, a total of four waves are involved — hence the term *four-wave mixing* (FWM). Discussions on holography and phase conjugation generally use different terminology, as summarized in Table 8.1.

Table 8.1 Comparison of terminology

Wave in Fig. 8.2	Holography	Phase Conjugation
O	Object wave	Signal wave
R	Reference wave	First pump wave
R^*	Reconstruction wave	Second pump wave
O^*	Phase conjugate of the object wave	Phase conjugate wave

In the present example, all the waves are at the same frequency, which is said to be the degenerate case. In the nondegenerate case, a phase conjugate wave is generated by mixing waves of different frequencies.

8.3 EXPRESSIONS FOR PHASE CONJUGATE WAVES

The expression for the phase conjugate wave will be explained taking a spherical wave as an example. The expression for a diverging spherical wave is

$$E_s(r, t) = \text{Re } E(r, \omega)e^{-j\omega t} \tag{8.2}$$

where

$$E(r, \omega) = \frac{A_0}{r}e^{jkr+j\phi} \tag{8.3}$$

and where A_0 is a constant real number.

The phase conjugate wave $E_{\text{pc}}(r, t)$ of this signal wave is obtained by performing the conjugation operation on every term except the temporal term, namely,

$$E_{\text{pc}}(r, t) = \text{Re } [E^*(r, \omega)e^{-j\omega t}] \tag{8.4}$$

where

$$E^*(r, \omega) = \frac{A_0}{r}e^{-jkr-j\phi} \tag{8.5}$$

The term e^{-jkr}/r indicates a converging spherical wave (see Section 1.5.4). The phase conjugation converts a diverging spherical wave into a converging spherical wave, and vice versa.

The phase conjugate wave is sometimes called a time-reversed wave. If the sign of the temporal term in Eq. (8.2) is reversed, that is, $t \to -t$, then

$$E_{\text{pc}}(r, t) = \text{Re } \left(\frac{A_0}{r}e^{j\omega t+jkr+j\phi}\right) \tag{8.6}$$

which is identical to $E_{\text{pc}}(r, t)$ given by Eq. (8.4). This means that $E_{\text{pc}}(r, t)$ is obtained by reversing the time. $E_{\text{pc}}(r, t)$ is like a motion picture played backward.

It is important to understand the meaning of ϕ. Let us compare the phases between two diverging spherical waves with and without ϕ. From Eqs. (8.2) and (8.3), these spherical waves are given by

$$E_s(r, t) = \text{Re } \left(\frac{A_0}{r}e^{-j\omega t+jkr+j\phi}\right) \tag{8.7}$$

$$E_d(r, t) = \text{Re } \left(\frac{A_0}{r}e^{-j\omega t+jkr}\right) \tag{8.8}$$

The waves are observed at a particular radius $r = r_0$. The phase of $E_s(r, t)$ at $t = t$ is identical to the phase of $E_d(r, t)$ at $t = t - \phi/\omega$. This means that the phase of $E_s(r, t)$

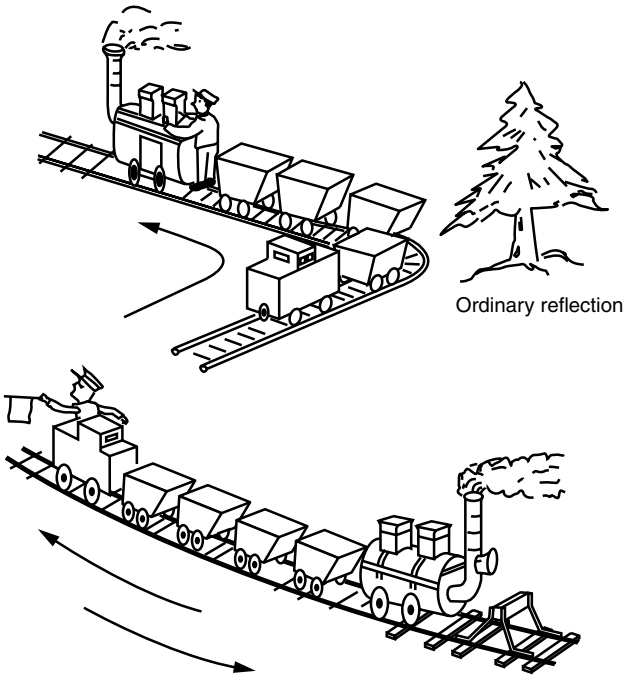

Comparison of ordinary reflection and phase conjugate reflection.

is equal to the phase that $E_d(r, t)$ had ϕ/ω seconds earlier. Thus, ϕ means that the phase of $E_s(r, t)$ is delayed from that of $E_d(r, t)$ by ϕ radians.

On the other hand, when the phase conjugate waves with and without ϕ are compared, the corresponding expressions are

$$E_{\text{pc}}(r, t) = \text{Re}\left(\frac{A_0}{r} e^{-j\omega t - jkr - j\phi}\right) \tag{8.9}$$

$$E_c(r, t) = \text{Re}\left(\frac{A_0}{r} e^{-j\omega t - jkr}\right) \tag{8.10}$$

The phase of $E_{\text{pc}}(r, t)$ at $t = t$ is equal to the phase that $E_c(r, t)$ will have at $t = t + \phi/\omega$. Hence, ϕ means that the phase of $E_{\text{pc}}(r, t)$ is leading by ϕ radians.

In conclusion, the phase conjugate wave propagates in the reverse direction of the signal wave. The phase is also reversed and if the phase of the signal wave is *delayed* by ϕ radians, then that of the phase conjugate wave is *leading* by ϕ radians. This is just like a train reversing its direction. The trailing coach becomes the leading coach if the phase is compared to the location of the coach.

8.4 PHASE CONJUGATE MIRROR FOR RECOVERING PHASEFRONT DISTORTION

One of the most important applications of the phase conjugate mirror is for eliminating wavefront distortion incurred during light transmission through a turbulent atmosphere

or dispersive optical fiber. The holographic principle will be used for explaining the recovery of the wavefront free from distortion.

First, the amount of fringe pattern shift due to the phase shift of the incident wave will be calculated. Figure 8.3a shows the fringe pattern formed by two counterpropagating plane waves:

$$E_1 = A_1 e^{-j\omega t + jkz} \tag{8.11}$$

$$E_2 = A_2 e^{-j\omega t - jkz} \tag{8.12}$$

If the amplitudes are equal, $A_1 = A_2 = A$, then the sum of $E_1 + E_2$ can be expressed as

$$E_1 + E_2 = 2Ae^{-j\omega t} \cos kz \tag{8.13}$$

The intensity peaks of Eq. (8.13) appear at every half-wavelength, as shown by the solid lines in Fig. 8.3a. Let us focus our attention on the particular peak at the center $z = 0$ in order to find how much the peak moves when one of the two waves shifts its phase. Let us say the phase of the forward wave E_1 is delayed by ϕ radians, and

$$E_1' = A_1 e^{-j\omega t + jkz + j\phi} \tag{8.14}$$

The interference pattern between E_1' and E_2 then becomes

$$E_1' + E_2 = 2Ae^{-j\omega t + j\phi/2} \cos(kz + \phi/2) \tag{8.15}$$

Peaks appear when the value inside the parentheses in Eq. (8.15) is zero, and the new location of the center peak is at

$$\Delta z = -\frac{1}{k}\frac{\phi}{2} \tag{8.16}$$

As a matter of fact, all peaks shift by Δz toward the left or toward the source of the delayed incident wave, as indicated by the dashed lines in Fig. 8.3a. This shift of the fringe pattern plays an important role in recovering the wavefront free from distortion.

Figure 8.3b explains how the wavefront disrupted by passing through a distorting medium is restored by means of the phase conjugate mirror. Let us say a plane wave whose wavefront is represented by the solid line in Fig. 8.3b(i) is incident from the left to the right. A rectangular shaped distorting medium whose refractive index is larger than that of the surrounding medium is placed in the way. The portion of the wavefront that has passed through the distorting medium is delayed, and the shape of the wavefront upon leaving the distorting medium becomes indented and resembles the letter C, as indicated by the solid line in Fig. 8.3b(ii). A hologram is generated from this distorted wavefront O and the reference wave R originating from point r. The recorded fringes in the hologram have protrusions shaped like the letter C in their pattern. The direction of the protrusion is toward the source of the incident wave as explained using Fig. 8.3a.

Next, consider the case when this hologram is illuminated by the pump wave R^* from the point source r'. Compare the ray that is reflected from the protruding

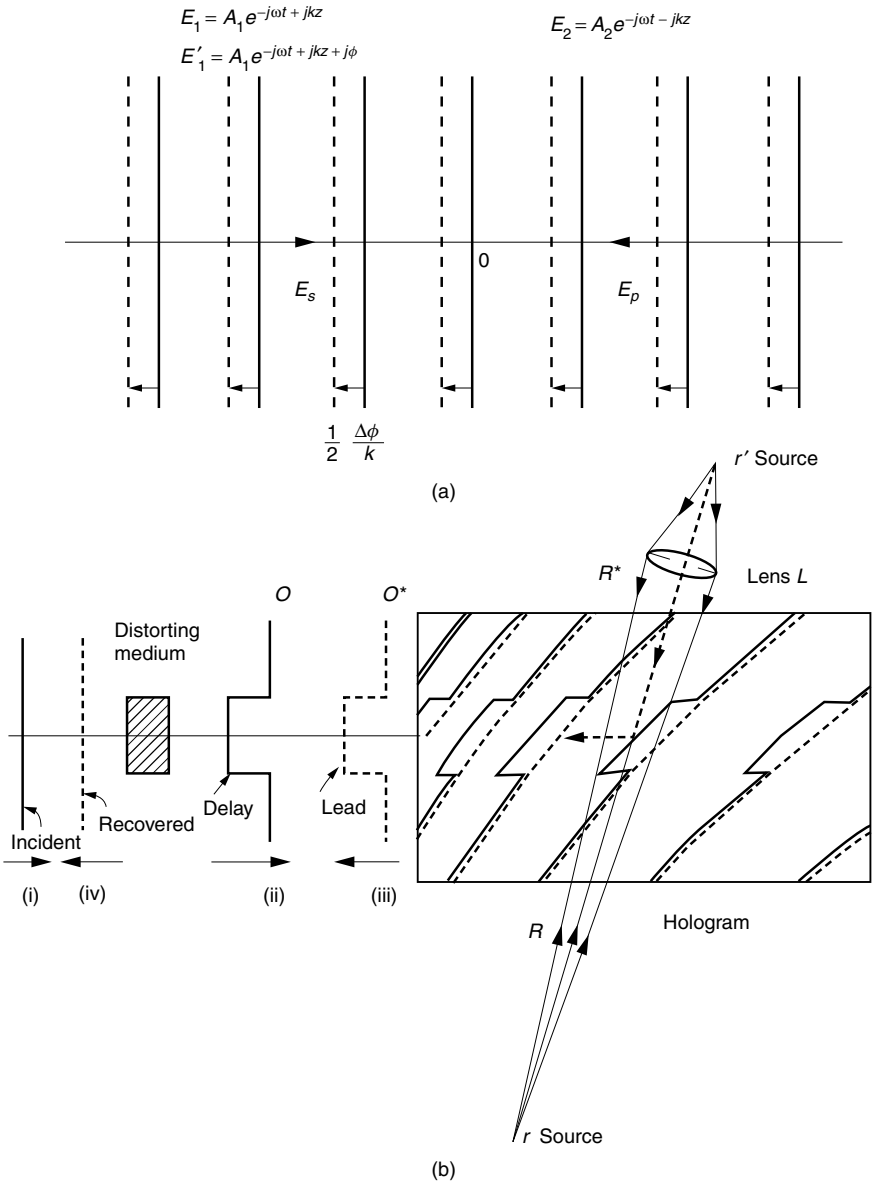

Figure 8.3 A phase conjugate wave is restored from the influence of a phase-distorting medium. (a) Fringe pattern formed by two counterpropagating plane waves. (b) Explanation of how the wavefront disrupted by passing through a distorting medium is restored by means of the phase conjugate mirror.

section of the small mirror and the ray reflected from the nonprotruding section. Not only does the ray reflected from the protruding section reach the mirror sooner, but also the point of reflection is shifted toward the left, and the wavefront O^* reflected from the hologram has a C-shaped dent as indicated by the dashed line in Fig. 8.3b(iii).

The shapes of the indentation in the O wave in Fig. 8.3b(ii) and the O^* wave in Fig. 8.3b(iii) are the same, but the difference is in their direction of propagation. They

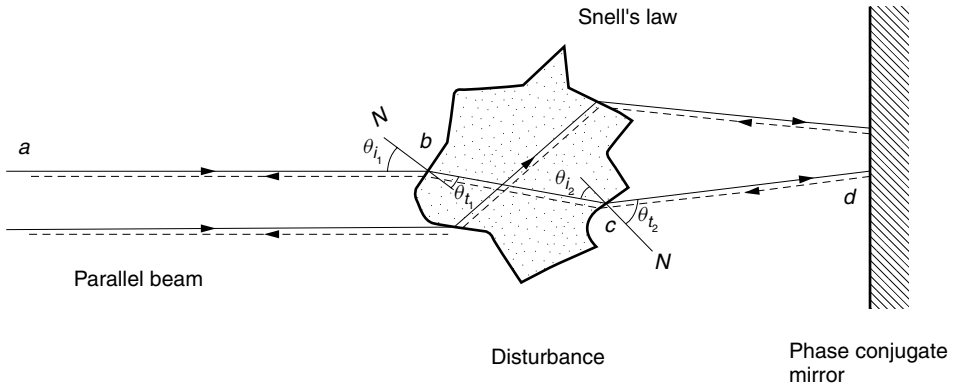

Figure 8.4 Recovery of the original parallel beam from a disturbed beam by means of a phase conjugate mirror. ___, Signal beam. - - - -, Phase conjugate beam.

are propagating in opposite directions, and the indented part of the O wave is delayed, but that of the O^* wave is in the lead.

If the O^* wave continues to propagate to the left and passes through the same distorting medium again, only the distorted portion of the wavefront is delayed, and the wavefront of the emerging wave recovers from the distortion, as indicated by the dashed line in Fig. 8.3b(iv).

Next, let us consider the more general case where the distorting medium has an irregular shape, as shown in Fig. 8.4. The particular ray path *abcd* is examined. At point *d*, the nature of the phase conjugate mirror directs the reflected wave exactly toward the direction from which it came. Once this direction of the retrace is set at point *d*, the rest of the paths are solely determined by Snell's refraction law. Snell's law is reciprocal, which means that regardless of whether the ray goes from left to right or right to left, it takes the same path. Thus, the reflected ray takes the path of *dcba*, which is exactly the reversal of *abcd*, and the reflected wave becomes an undistorted parallel beam.

8.5 PHASE CONJUGATION IN REAL TIME

In the previous sections, in order to explain the method of generating a phase conjugate wave, a photographic film was used as the recording medium. For most applications, however, it is unrealistic to wait for the film to be developed. For real-time operation, the film has to be replaced by a more suitable recording medium. Third order nonlinear media are used. The refractive indices of such media change in real time when exposed to light [3,4].

The most commonly used materials are photorefractive crystals such as $BaTiO_3$, $LiNbO_3$, $LiTaO_3$, and $Bi_{12}SiO_{20}$ (BSO). These photorefractive crystals have a large nonlinear susceptibility, and the values of χ_{eff} are in the range of 10^{-20}–$10^{-23}(\text{V/m})^2$. The light intensity required to produce a noticeable effect can be as small as 1 mW/cm^2, which means lasers with output powers of the order of tens of milliwatts will suffice. The drawback with these crystals is the slow response time, which ranges from a few seconds to hours.

Nonlinear Kerr media such as glass, calcite, YAG, sapphire, benzene, liquid crystal, and semiconductors are an alternative to photorefractive crystals. Semiconductors like chromium-doped gallium arsenide (GaAs:Cr), iron-doped indium phosphide (InP:Fe), or titanium-doped indium phosphide (InP:Ti) change their energy band gap when illuminated by high-intensity light and hence change their refractive index. Their nonlinear susceptibility is low and $\chi_{\text{eff}} = 10^{-22}-10^{-32}(\text{V/m})^2$, but the response time is as fast as $10^{-8}-10^{-12}$ seconds.

Yet another possibility are materials that display either stimulated Brillouin scattering (SBS) or stimulated Raman scattering (SRS). Examples of such materials are gaseous methane (CH_4), carbon dioxide (CO_2), liquid carbon disulfide (CS_2), alcohol (C_2H_5OOH), and glass. The magnitude of χ_{eff} is $10^{-32}-10^{-34}(\text{V/m})^2$ and the response time is $10^{-8}-10^{-9}$ seconds.

8.6 PICTURE PROCESSING BY MEANS OF A PHASE CONJUGATE MIRROR

If the distorting medium in Fig. 8.3b is replaced by an inhomogeneous medium such as turbulent air, the system in Fig. 8.3b can be used immediately for correcting a distorted image.

Figure 8.5 shows an arrangement for compensating for the distortion caused by transmission of the signal light through an in homogeneous medium. Referring to Fig. 8.5, a light source illuminates the input mask, and the signal light from the input mask undergoes distortion as it passes through the turbulent air. The distorted signal is incident onto the phase conjugate mirror. The signal light reflected from the phase conjugate mirror reverses the sign of its phase. By going through the same inhomogeneous medium a second time, the distortion in the reversed phase is exactly canceled. The corrected wavefront reaches the image plane by way of the half-mirror. The location of the image plane is set such that the total distance between the input mask to the phase conjugate mirror is identical to that between the phase conjugate mirror and the image plane.

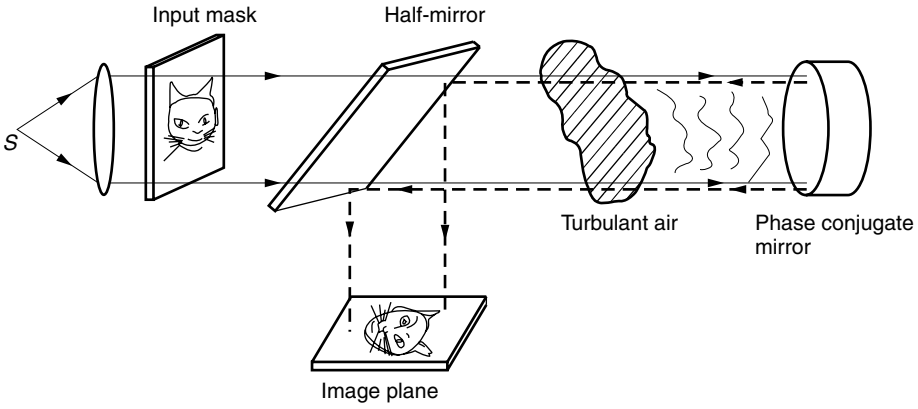

Figure 8.5 Arrangement designed to compensate for the wavefront distortion incurred during transmission through turbulent air.

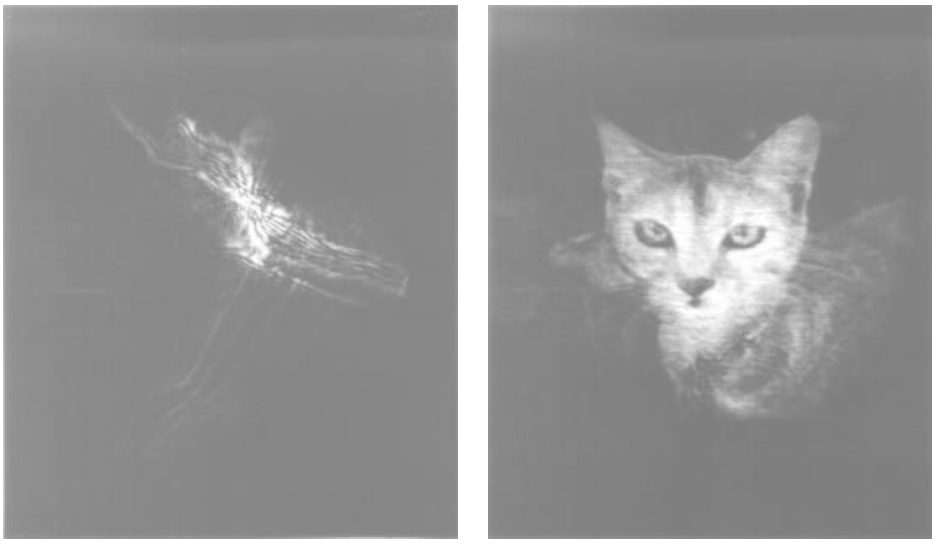

(a) (b)

Figure 8.6 Image restoration by means of a phase conjugate mirror. (a) Image through a distorted sheet of glass. (b) Image restored by means of a phase conjugate mirror. (Courtesy of J. Feinberg [5].)

It is important to realize that the wavefront has to retrace the same inhomogeneity. For this to be true, the air turbulence has to be stationary for the duration of the round trip of the signal light through the air turbulence.

Figure 8.6 shows the result of an experiment to demonstrate the effectiveness of compensation using such an arrangement as shown in Fig. 8.5 [5,6]. A sheet of surface-distorted glass was used instead of turbulent air. Figure 8.6a shows the image obtained using an ordinary mirror in place of the phase conjugate mirror. Figure 8.6b shows the restored image of the cat obtained using the phase conjugate mirror.

The arrangement shown in Fig. 8.5 has another application. By removing the inhomogeneous medium it can be used as a photolithography machine. The image of the input mask can be projected onto a substrate in the image plane. The system not only does away with imaging lenses but also avoids direct contact of the input mask with the substrate.

8.7 DISTORTION-FREE AMPLIFICATION OF LASER LIGHT BY MEANS OF A PHASE CONJUGATE MIRROR

The same principle for compensating distortion caused by inhomogeneity in Fig. 8.5 can be used to construct a light amplifier whose output light is free from distortion [7]. Problems of inhomogeneity normally occur within a high-power semiconductor laser amplifier. This can be compensated using the arrangement shown in Fig. 8.7, which is nothing but a modification of Fig. 8.5.

Figure 8.7a shows a semiconductor laser without compensation. The inhomogeneity of the amplifier generates wavefront distortion in the output light. In Fig. 8.7b, a phase conjugate mirror is placed in the amplified output light. The reflected phase conjugate

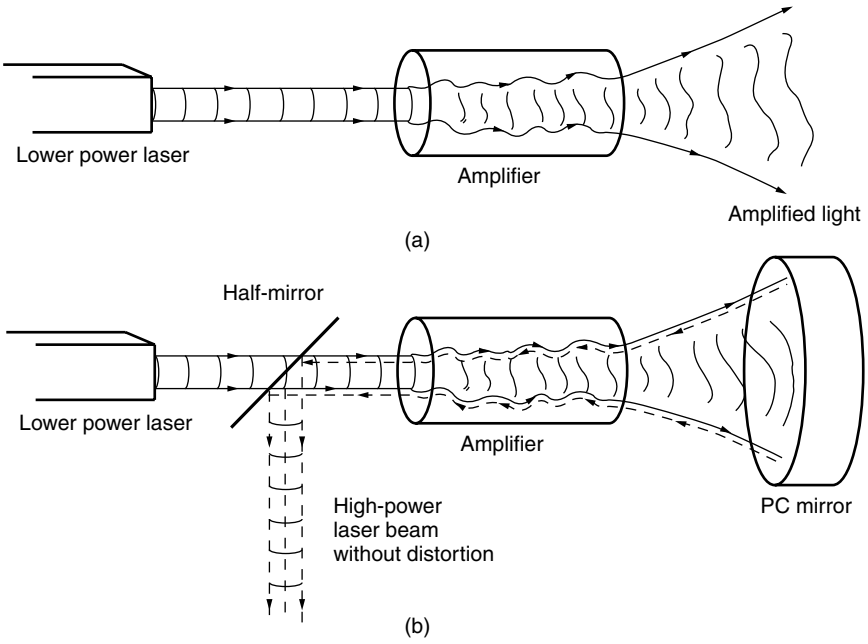

Figure 8.7 Compensation of distortion with phase conjugate (PC) mirror. (a) Amplification of light with distortion. (b) Amplification of light without distortion.

wave retraces through the inhomogeneity in the amplifier and takes the path of the original laser beam without distortion. The distortion-free amplified output exits by way of the half-mirror.

8.8 SELF-TRACKING OF A LASER BEAM

By nature, the phase conjugate wave retraces the path to the original source. Making use of this property, optical tracking or self-targeting systems can be realized [1,7].

Figures 8.8 –8.10 show examples of such systems.

Figure 8.8 shows an arrangement for directing a high-intensity laser beam to a point target. The target is illuminated by a laser. A portion of the light scattered by the target is intercepted by the optical amplifier and is amplified. The amplified output is incident onto the phase conjugate mirror. The reflected phase conjugate wave enters the optical amplifier again. The output from the amplifier is not only amplified twice but also converges to the point target. In Fig. 8.9, several self-targeting systems are combined to achieve super-high-intensity light concentrated on a single target with the goal of initiating thermal fusion of the pellet target. As long as the depth of the phase conjugate mirror is longer than the longest path differences among the targeting systems, the pulses from each system coincide at the pellet target and provide super-high-intensity light to the target.

Figure 8.10 shows another example of a tracking system [8]. This time, however, the arrangement is slightly different. Site A sends out a pilot light S through a turbulent medium to Site B. The pilot light contains information about the turbulence. At Site B,

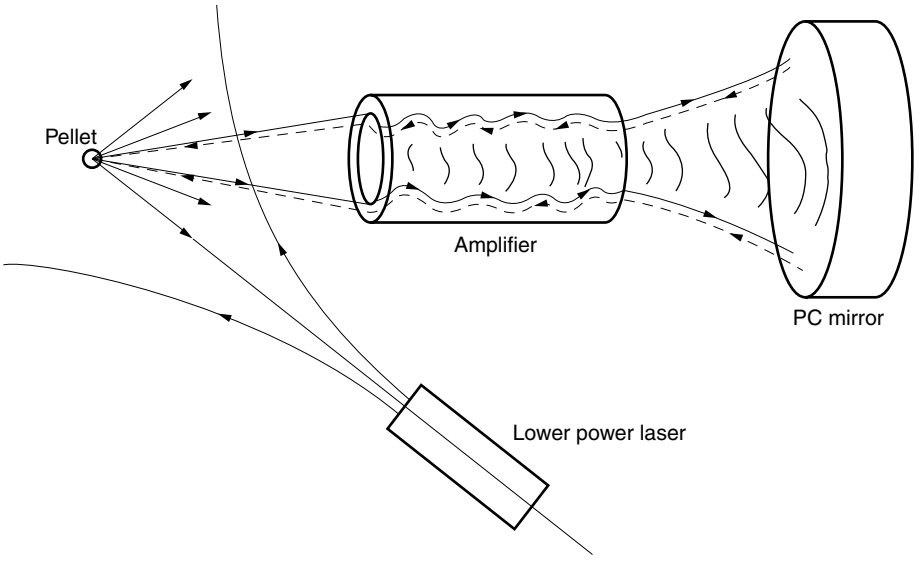

Figure 8.8 Optical self-targeting by means of a phase conjugate (PC) mirror. (After V. V. Shkunov and B. Ya Zel'dovich [7].)

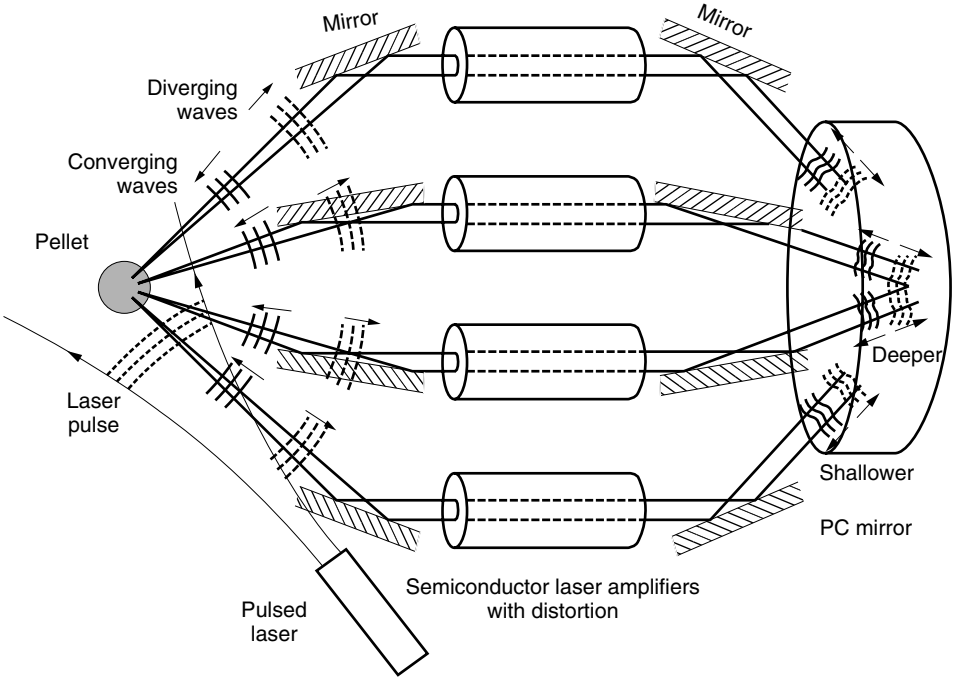

Figure 8.9 Synchronized pulses from parallel amplifiers. (After D. M. Pepper [3].)

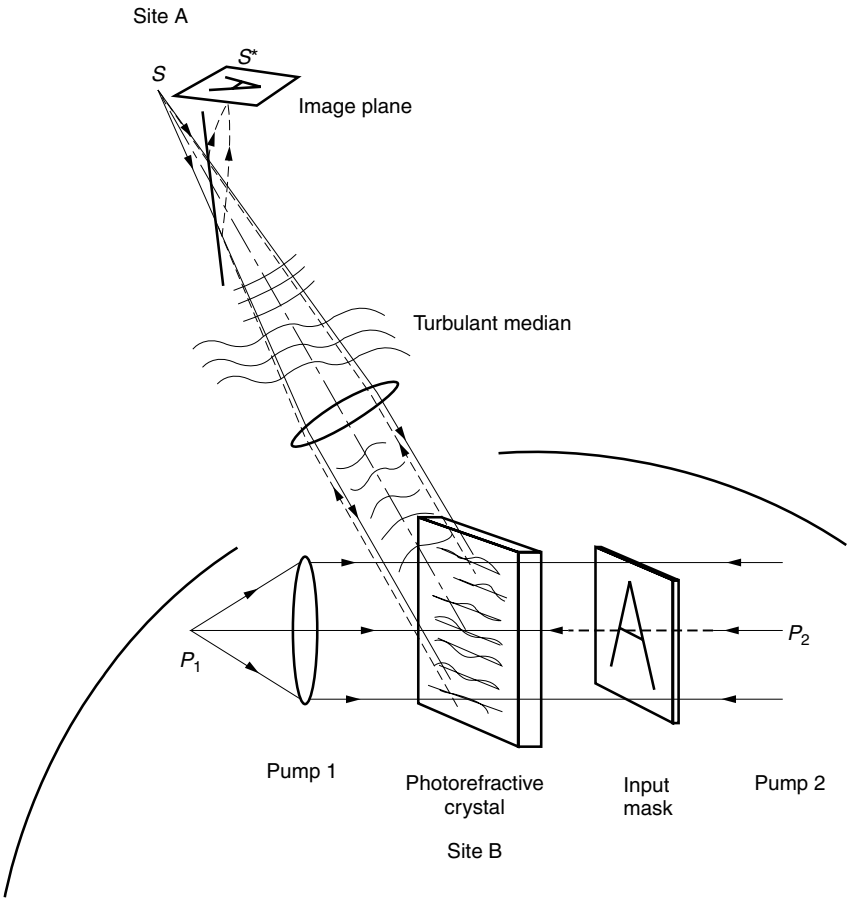

Figure 8.10 Tracking source with one-way transmission through turbulance. (After B. Fischer et al. [8].)

the pilot light is mixed with the pump wave P_1 to form a holographic fringe pattern in a photorefractive crystal.

The information signal, a picture of the letter A, is to be sent back from Site B, passing through the same turbulent medium to Site A. Pump beam P_2 propagating in the opposite direction from P_1 illuminates the input mask of the letter A and then illuminates the holographic fringes. The wave S^* diffracted from the holographic fringes is the phase conjugate wave of the source wave S that has come through the turbulence. S^* goes through the turbulence and the original wavefront is recovered and propagates toward Site A. The letter A will be imaged at Site A.

In the previous arrangements, the signal wave had to go through the turbulence twice, but what is unique about the present arrangement is that the signal wave goes through the turbulence once and the pump wave goes through once. It is a more practical configuration for transmitting information over a distance.

An interesting modification is that if the mask of the letter A is replaced by a fast-speed electronic shutter, then pump wave P_2 is temporally modulated and a free-space optical communication link immune to turbulence is established.

Another application of the self-tracking capability of the phase conjugate wave is the adaptive fiber coupler. The adaptive fiber coupler is a coupler that does not need critical alignment between the two connecting fibers [9]. Figure 8.11a shows the geometry of the coupling. A photorefractive crystal such as barium titanate ($BaTiO_3$) is placed inside an optical resonator formed by a pair of ordinary mirrors. Mirror M_1 is placed on one side of the crystal. A partially reflecting mirror M_2 has been deposited on the facet of fiber 2. M_2 is arranged to be parallel to M_1 so as to form an optical resonator. Light incident from fiber 1 is scattered by impurities in the crystal. The lightwave scattered in the direction perpendicular to mirrors M_1 and M_2 bounces back and forth between M_1 and M_2. Let the wave going horizontally from left to right be the pump wave P_1 and that going from right to left be pump wave P_2.

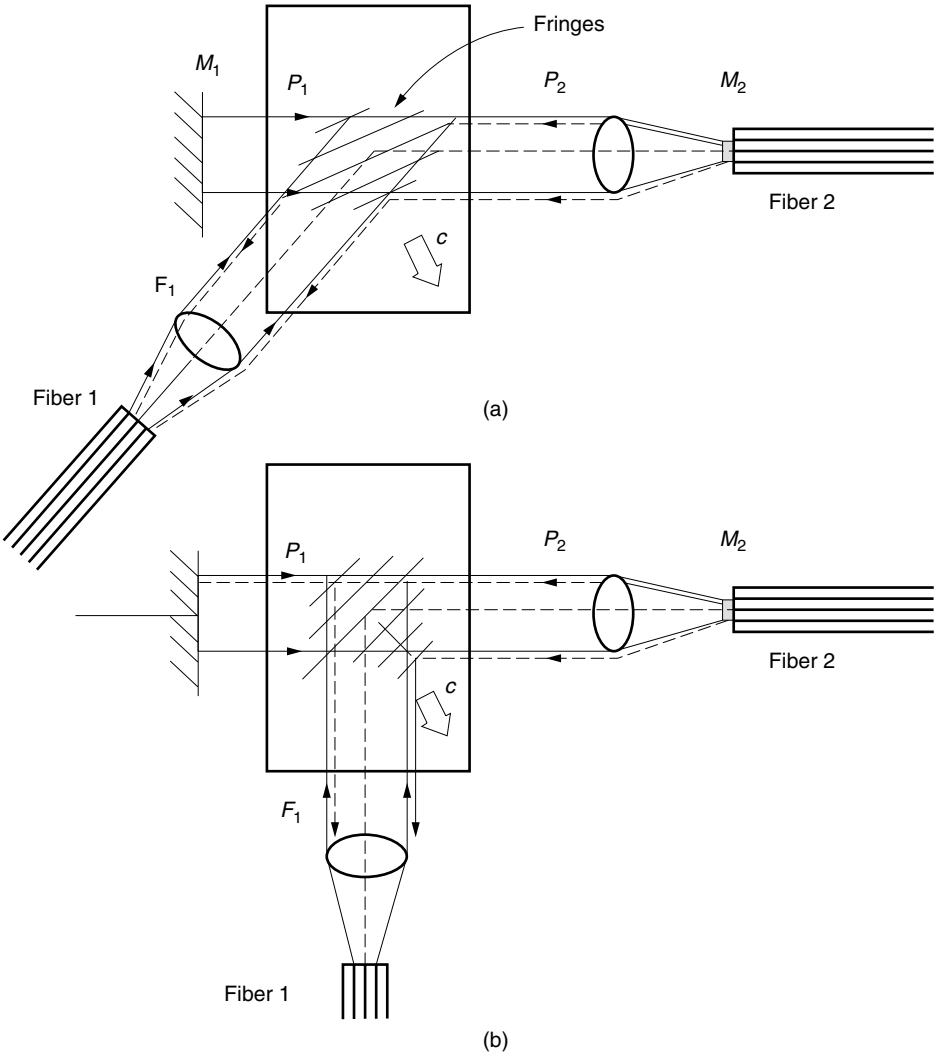

Figure 8.11 Adaptive fiber coupler. (a) Coupling between fibers 1 and 2. (b) When fiber 1 is moved, coupling adaptively continues.

Note that there is no external pump wave in this configuration. There is a special reason for using the photorefractive crystal as the phase conjugate element. For instance, when a nonlinear Kerr medium such as calcite is used, the recorded fringe pattern is an exact replica of the interference pattern of the incident lightwaves. However, when a photorefractive medium like $BaTiO_3$ is used, the recorded fringe pattern is shifted from that of the interference pattern of the incident lightwaves because, as mentioned in Section 5.7.2, the change in refractive index is proportional to the spatial derivative of the light intensity rather than the light intensity itself. Because of this fringe pattern shift, when two beams of equal intensity cross in a photorefractive medium as shown in Fig. 8.12a, the two outputs are uneven and the power at d is larger than at b. The energy is pulled toward the direction of the crystal axis c of the crystal. This is called the two-wave mixing gain of a photorefractive material.

With the configuration shown in Fig. 8.11, the light energy is preferentially bent toward M_2. This method of generating a conjugate wave without external pump waves is called self-pumped phase conjugation (SPPC).

Figures 8.12b and 8.12c show a few more SPPC configurations of the conjugate mirrors. In Fig. 8.12b, the walls of the crystal replace the external mirrors. Figure 8.12c makes use of total internal reflection at the crystal walls [10,11]. The SPPC configurations have significant practical value.

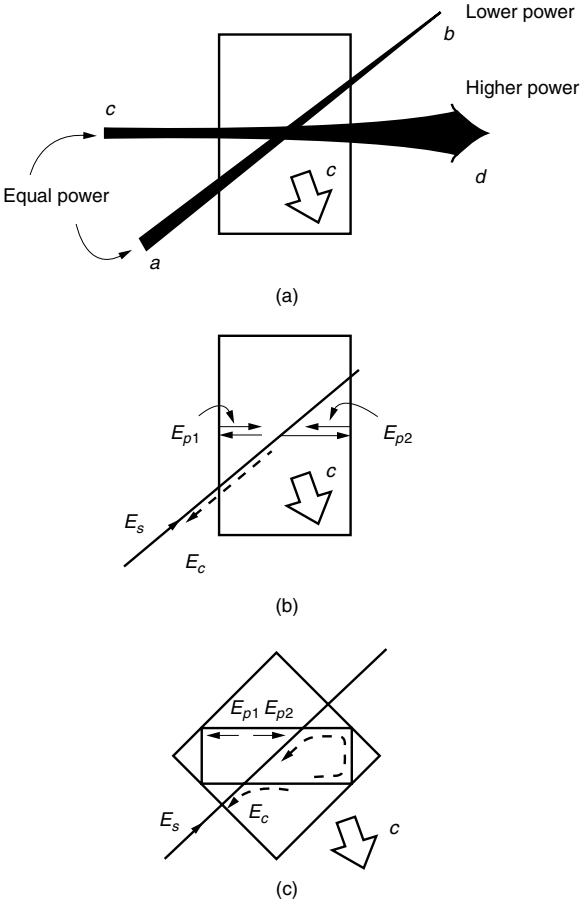

Figure 8.12 Self-pumped phase conjugation. (a) The direction of the energy transfer. (b) SPPC without external cavity. (c) SPPC with total internal reflection.

The incident light F_1 from fiber 1 and pump wave P_1 start forming holographic fringes. The direction of the fringes is such that the incident wave F_1 from fiber 1 is directed toward the input facet of fiber 2 and the connection is made between fibers 1 and 2.

If a misalignment of fiber 1 takes place, as shown in Fig. 8.11b, the direction of the fringe pattern in the crystal rotates such that F_1 is still reflected toward fiber 2. There is, however, a decrease in the energy transfer into the optical resonator. As the bisect between F_1 and P_1 moves away from the crystal axis, the diffraction efficiency from the photorefractive crystal decreases.

It should be noted that no external pump light is necessary in this coupler. The light F_1 from fiber 1 is transferred to the pump waves, and light energy pours into the optical resonator from the light F_1 of fiber 1.

8.9 PICTURE PROCESSING

By combining a pair of phase conjugate mirrors and a multiexposed hologram, an associative memory system such as shown in Fig. 8.13 can be constructed. The system can identify which one of a collection of memorized pictures best fits the interrogating obscure picture [12].

Let us say that the memorized pictures are of a cat, a dog, and a monkey. In memorizing these animal pictures, the angle of incidence of the reference beam is changed each time the input picture is exposed to the photographic film. Let us say the incident angle of reference beam R_1 used for recording the cat O_1 is at 10° from the normal to the photographic film. Reference beam R_2 used for recording the dog O_2 is at 20°, and reference beam R_3 used for the monkey O_3 is at 30°. After all three exposures are completed, the photographic film is developed and placed in the system shown in Fig. 8.13b.

The operation of the system will be explained with a picture of a cat as the interrogating picture. The transmittance t of the multiexposed hologram is

$$\begin{aligned} t &= \beta \sum_{i=1}^{3} (R_i + O_i)(R_i^* + O_i^*) \\ &= \beta \sum_{i=1}^{3} (|R_i|^2 + |O_i|^2 + R_i^* O_i + R_i O_i^*) \end{aligned} \tag{8.17}$$

where β is a constant characterizing the photographic film. Only the fourth term,

$$t_4 = \beta \sum_{i=1}^{3} R_i O_i^* \tag{8.18}$$

is of concern. When the hologram is illuminated by the light pattern O_1 of the cat, the output light from the hologram is

$$t_4 O_1 = \beta (R_1 O_1^* O_1 + R_2 O_2^* O_1 + R_3 O_3^* O_1) \tag{8.19}$$

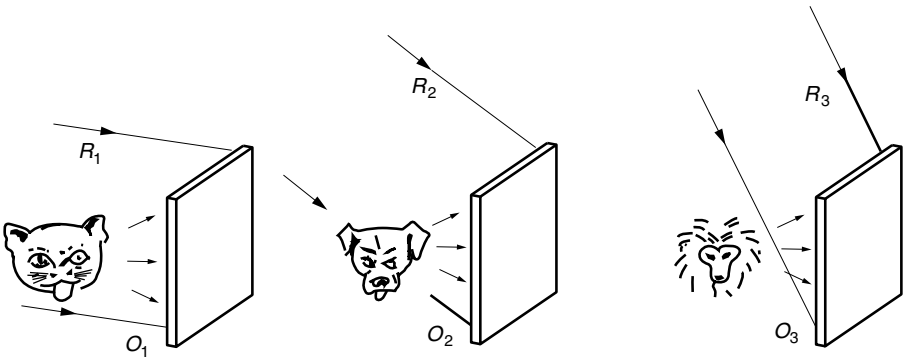

(a)

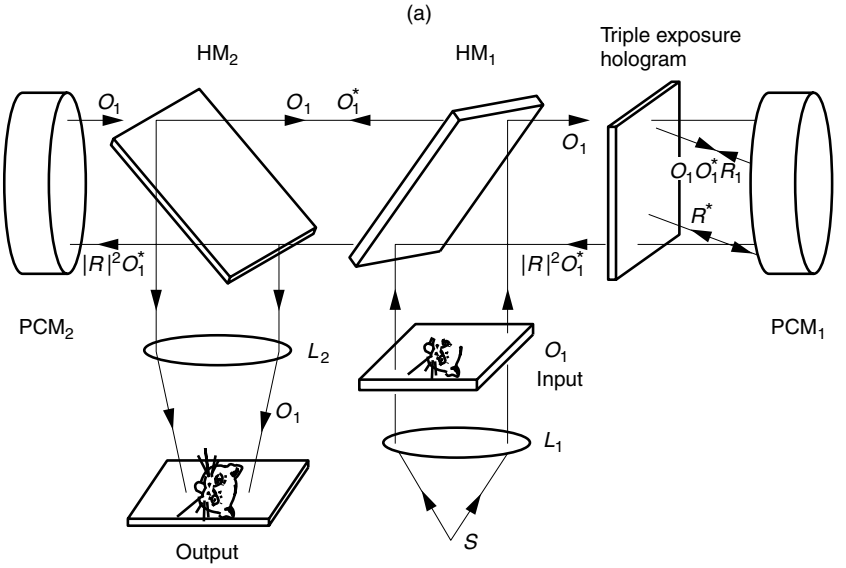

(b)

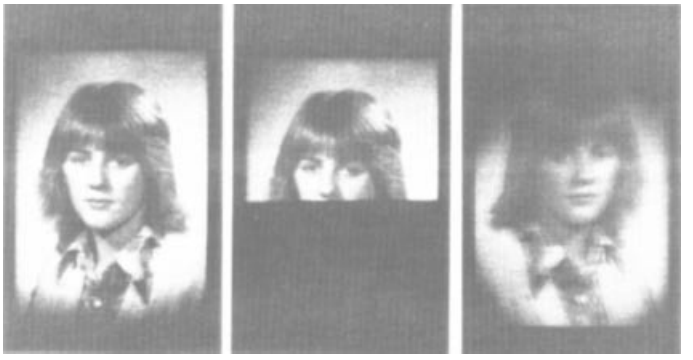

(i) Image stored in memory (ii) Incomplete input image (iii) Associated output image

(c)

Figure 8.13 Associative memory system. (a) Multi-exposed hologram. Three exposures are made on the same hologram. At each exposure, the direction of the reference beam is changed. (After D. M. Pepper [3].) (b) Interrogation of the input image. (c) With a portion of the portrait as the input, the image of the entire face is recovered. (Courtesy of Y. Owechko et al. [12].)

The first term predominates in Eq. (8.19), because not only do the amplitude distributions of O_1 and O_1^* match, but also the phase angle of $O_1^* O_1$ is constant (zero) throughout the pattern. The output $t_4 O_1$ from the hologram is essentially R_1 with reduced intensity.

Beam R_1 emergent from the hologram is now reflected by the right-hand-side phase conjugate mirror and the reflected beam becomes R_1^*. The hologram is now reilluminated by R_1^*. The contribution of the fourth term in Eq. (8.17) to the light transmitted through the hologram is

$$t_4 R_1^* = \beta(O_1^* R_1 R_1^* + O_2^* R_2 R_1^* + O_3^* R_3 R_1^*) \tag{8.20}$$

The contribution of the first term of Eq. (8.20) is predominant because the phase angle of $R_1 R_1^*$ is exactly zero, while that of $R_2 R_1^*$ is 10° and that of $R_3 R_1^*$ is 20° and propagates off axis. The emergent beam from the hologram becomes O_1^*.

O_1^* is further converted into O_1 by the phase conjugate mirror on the left-hand side and finally reaches the output image plane by way of the half-mirror HM_2. The image of the cat is formed by means of the imaging lens L_2. The beam that passes through the half-mirror HM_2 will repeat the same process to enhance the sensitivity of the system.

The sensitivity of the system can be improved significantly if a photographic film with a thick emulsion is used for fabricating the hologram. The sensitivity of the brightness of the reconstructed image to the angle of incidence of the reconstructing beam is enhanced due to the increased sizes of the miniature mirrors in the fringe pattern in the emulsion [2]. In fact, if the photographic film is replaced by a volume holographic material such as a $BaTiO_3$ crystal, a significant improvement in sensitivity and flexibility is achieved.

The power of discrimination can be adjusted by the threshold level of the phase conjugate mirror, and even a picture of the cat's brother or a faded imperfect input image can still be interrogated. Such a system is useful for interrogating handwritten letters or for fingerprint detection.

Figure 8.13c gives a similar demonstration for a portrait. Using only a portion of the portrait as input, the entire portrait is generated as a result of the interrogation.

8.10 THEORY OF PHASE CONJUGATE OPTICS

The theory of phase conjugate optics will be presented. Even though the level of treatment is elementary, it is still useful for solving practical problems.

8.10.1 Maxwell's Equations in a Nonlinear Medium

Maxwell's equations are the starting point for the quantitative representation of nonlinear phenomena [13–19]. Maxwell's equations are repeated here for convenience:

$$\nabla \times \mathbf{E} = -\frac{\partial \mathbf{B}}{\partial t} \tag{8.21}$$

$$\nabla \times \mathbf{H} = \mathbf{J} + \frac{\partial \mathbf{D}}{\partial t} \tag{8.22}$$

$$\nabla \cdot \mathbf{D} = \rho \tag{8.23}$$

$$\nabla \cdot \mathbf{B} = 0 \tag{8.24}$$

where

$$\mathbf{D} = \epsilon_0 \mathbf{E} + \mathbf{P} \tag{8.25}$$

$$\mathbf{B} = \mu_0 \mathbf{H} + \mathbf{M} \tag{8.26}$$

P is the induced electric polarization and is the focus of attention in this chapter. The medium is assumed to be nonconducting and nonmagnetic. This assumption leads to

$$\mathbf{J} = \rho = \mathbf{M} = 0 \tag{8.27}$$

From Eqs. (8.21), (8.22), (8.25), and (8.27), the following expression is obtained:

$$\nabla \times \nabla \times \mathbf{E} + \frac{1}{c^2} \frac{\partial^2 \mathbf{E}}{\partial t^2} = -\mu_0 \frac{\partial^2 \mathbf{P}}{\partial t^2} \tag{8.28}$$

where $c^2 = (\epsilon_0 \mu_0)^{-1}$. The identities involving differential operators that will be used to simplify Eq. (8.28) are

$$\nabla \times \nabla \times \mathbf{E} = \nabla(\nabla \cdot \mathbf{E}) - \nabla^2 \mathbf{E} \tag{8.29}$$

$$\nabla \cdot \mathbf{D} = \mathbf{E} \cdot \nabla \epsilon + \epsilon \nabla \cdot \mathbf{E} \tag{8.30}$$

If the spatial variation $\nabla \epsilon$ is negligible, then Eqs. (8.23), (8.27), and (8.30), lead to

$$\nabla \cdot \mathbf{E} = 0 \tag{8.31}$$

With Eqs. (8.29) and (8.31), Eq. (8.28) becomes

$$\nabla^2 \mathbf{E} - \frac{1}{c^2} \frac{\partial^2 \mathbf{E}}{\partial t^2} = \mu_0 \frac{\partial^2 \mathbf{P}}{\partial t^2} \tag{8.32}$$

Equation (8.32) can be interpreted as the wave equation of **E** whose source of excitation is $\mu_0 \partial^2 \mathbf{P} / \partial t^2$. However, the electric polarization **P** is induced by **E**; and **P** is

$$\mathbf{P} = \epsilon_0 (\boldsymbol{\chi}^{(1)} \cdot \mathbf{E} + \boldsymbol{\chi}^{(2)} : \mathbf{EE} + \boldsymbol{\chi}^{(3)} \vdots \mathbf{EEE} + \cdots) \tag{8.33}$$

The first term in Eq. (8.33) is proportional to **E**, while the rest of the terms are proportional to higher orders of **E**. The former is called the linear part $\mathbf{P}_{\mathrm{L}}$; and the latter, the nonlinear part $\mathbf{P}_{\mathrm{NL}}$ of the induced electric polarization

$$\mathbf{P} = \mathbf{P}_{\mathrm{L}} + \mathbf{P}_{\mathrm{NL}} \tag{8.34}$$

where

$$\mathbf{P}_{\mathrm{L}} = \epsilon_0 \boldsymbol{\chi}^{(1)} \cdot \mathbf{E} \tag{8.35}$$

$$\mathbf{P}_{\mathrm{NL}} = \epsilon_0 (\boldsymbol{\chi}^{(2)} : \mathbf{EE} + \boldsymbol{\chi}^{(3)} \vdots \mathbf{EEE} + \cdots) \tag{8.36}$$

$\boldsymbol{\chi}^{(i)}$ is the ith order optical susceptibility and is a tensor of rank $i + 1$. A nonlinear dielectric medium is characterized by $\mathbf{P}_{\mathrm{NL}}$.

Assuming a sinusoidal time dependence and substituting for $\mathbf{P}_{\mathrm{L}}$ from Eq. (8.35) and $\mathbf{P}_{\mathrm{NL}}$ from Eq. (8.36), the wave equation Eq. (8.32) becomes

$$\nabla^2\mathbf{E} + \left(\frac{\omega}{c}\right)^2 \mathbf{E} = -\mu_0\epsilon_0\omega^2\boldsymbol{\chi}^{(1)} \cdot \mathbf{E} + \mu_0 \frac{\partial^2 \mathbf{P}_{\mathrm{NL}}}{\partial t^2} \tag{8.37}$$

Noting that

$$\boldsymbol{\epsilon}_r = 1 + \boldsymbol{\chi}^{(1)} \tag{8.38}$$

Eq. (8.37) can be rewritten as

$$\nabla^2\mathbf{E} + k_0^2\boldsymbol{\epsilon}_r \cdot \mathbf{E} = \mu_0 \frac{\partial^2 \mathbf{P}_{\mathrm{NL}}}{\partial t^2} \tag{8.39}$$

with

$$k_0^2 = \omega^2\mu_0\epsilon_0 \tag{8.40}$$

8.10.2 Nonlinear Optical Susceptibilities $\chi^{(2)}$ and $\chi^{(3)}$

Susceptibilities with i larger than 3 are hardly used, so that only the properties of $\chi^{(2)}$ and $\chi^{(3)}$ are investigated here. Certain materials such as glass or NaCl have zero $\chi^{(2)}$ but have nonzero $\chi^{(3)}$. For experiments to be performed based solely on $\chi^{(3)}$, such materials are attractive because there are no second order nonlinearities, which might complicate the results. A slight detour will be taken to explain why some materials have zero $\chi^{(2)}$ but nonzero $\chi^{(3)}$.

First of all, for simplicity, let us choose

$$\mathbf{E} = (E\cos\omega t)\hat{\mathbf{x}} \tag{8.41}$$

Since only the $\hat{\mathbf{x}}$ component is considered, Eq. (8.41) can be treated as a scalar quantity. The second nonlinearity gives

$$P_{\mathrm{NL}}^{(2)} = \tfrac{1}{2}\chi^{(2)}E^2(1 + \cos 2\omega t) \tag{8.42}$$

and becomes the expression for second harmonic generation (SHG). On the other hand, the third nonlinearity gives

$$P_{\mathrm{NL}}^{(3)} = \tfrac{1}{4}\chi^{(3)}E^3(3\cos\omega t + \cos 3\omega t) \tag{8.43}$$

and generates the third order higher harmonic.

Generation of the higher harmonics will be examined graphically in order to find out why crystals with inversion symmetry do not display the second order nonlinearity [19].

Figure 8.14a shows a one-dimensional model of a crystal with inversion symmetry. It possesses an inversion symmetry with respect to any one of the ions. Let us say that with respect to the c axis $\oplus$ and $\ominus$ charges are symmetrically distributed. Consider an instant that the electric field $\mathbf{E}$ of the light is in the positive x direction. The positive charges move to the right, and the negative charges move to the left, as shown in

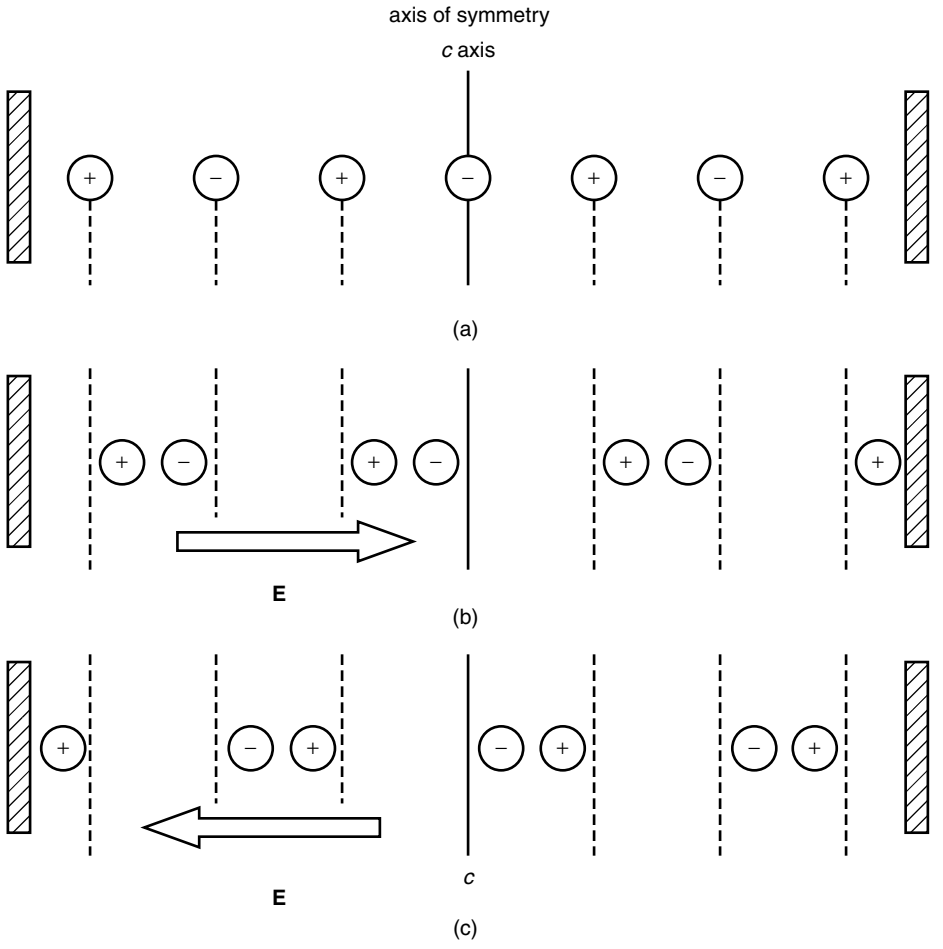

Figure 8.14 Induced electrical polarization in a crystal with inversion symmetry. (a) No light $\mathbf{E} = 0$. (b) Light is on with $\mathbf{E} = E\hat{\mathbf{x}}$. (c) Light is on with $\mathbf{E} = -E\hat{\mathbf{x}}$.

Fig. 8.14b. At the next instant, the direction of $\mathbf{E}$ is reversed, and each charge moves in the opposite direction and the distribution of the charges becomes like the one shown in Fig. 8.14c. The distribution of the charges that $\mathbf{E}$ sees is the same for both instances, and the amounts of polarization are the same, except for the reversal of the outermost charges that determine the polarization polarity.

Figure 8.15a shows a plot of P_{NL} with respect to time. Even though the shape is distorted from a sinusoidal curve due to the nonlinearity, the shape of the curve for positive values of polarization in the range $0 < t < T/2$ is identical to that for negative values of polarization in the range $T/2 < t < T$ except for its sign, where T is the period of the fundamental frequency.

If the second harmonic is present, the shapes in the first half and the second half cannot be identical, as will be illustrated using Fig. 8.15b in which the curves of the fundamental and the second harmonic are plotted. In the region $0 < t < T/2$, the signs of the peaks of the fundamental and second harmonic are both positive; while in the

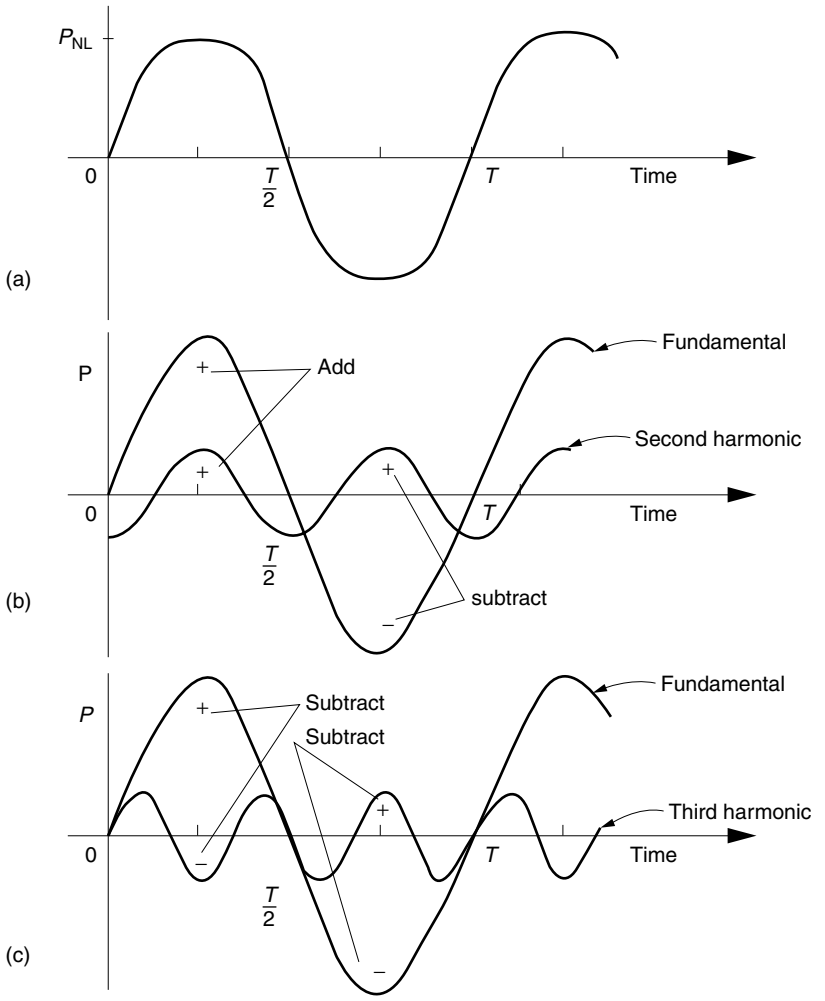

Figure 8.15 Graphical illustration that a crystal with inversion symmetry has zero $\chi^{(2)}$.

region $T/2 < t < T$, the peaks of the fundamental and second harmonic have opposite signs. As long as the second harmonic is added to the fundamental, the response curve cannot have the same shape in the regions $0 < t < T/2$ and $T/2 < t < T$, as shown in Fig. 8.15a for a crystal with inverse symmetry. Thus, the second order optical susceptibility $\chi^{(2)}$ has to be zero in a crystal with inversion symmetry.

The same crystal, however, can have a third order nonlinearity. Figure 8.15c shows the plot of the fundamental and the third harmonic. In the region $0 < t < T/2$, the center peak of the third harmonic is negative while that of the fundamental is positive. The resultant is the difference between these two peaks. In the region $T/2 < t < T$, the center peak of the third harmonic is positive while that of the fundamental is negative. The resultant is again the difference between the two peaks, and the shape in the region $0 < t < T/2$ becomes identical to that in $T/2 < t < T$. Thus, a crystal with inversion symmetry can support the third order nonlinearity.

In summary, a crystal with inversion symmetry cannot support the second order nonlinearity but can support the third order nonlinearity. Crystals that do not possess inversion symmetry can, in principle, support simultaneously second and third order nonlinearities.

In the next section, we return to solving the nonlinear Maxwell's equation.

8.10.3 Coupled Wave Equations

The first step toward solving the nonlinear Maxwell's equation, Eq. (8.39), is to find an expression for $\mathbf{P}_{\text{NL}}$ in Eq. (8.39). In the general case of four-wave mixing, $\mathbf{P}_{\text{NL}}$ is generated from a combination of four incident waves of different frequencies.

The analytic signal is one of the most common ways of solving differential equations in electrical engineering. A sinusoidal function, say, $\cos \omega t$, is replaced by the exponential $e^{j\omega t}$ and the differential equations are solved. The final answer is obtained by taking only the real part of the solution. This method does not necessarily work for solving problems in nonlinear optics; therefore, $\cos \omega t = \frac{1}{2}(e^{j\omega t} + \text{c.c.})$ will be used. See the boxed note and Appendix B of Volume 1.

All incident waves are assumed to be plane waves and are made up of four waves:

$$\mathbf{E}(\mathbf{r}, t) = \sum_{j=1}^{4} \hat{\mathbf{a}}_j |A_j(\mathbf{r}, \omega_j)| \cos(-\omega_j t + \mathbf{k}_j \cdot \mathbf{r} + \phi_j) \tag{8.44}$$

where $\hat{\mathbf{a}}_j$ are the unit vectors of the direction of polarization. The exponential expression that is exactly equivalent to Eq. (8.44) is

$$\mathbf{E}(\mathbf{r}, t) = \frac{1}{2} \sum_{j=1}^{4} \hat{\mathbf{a}}_j [E_j(\mathbf{r}, \omega_j) e^{-j\omega_j t} + \text{c.c.}] \tag{8.45}$$

where

$$E_j(\mathbf{r}, \omega_j) = A_j(\mathbf{r}, \omega_j) e^{j\mathbf{k}_j \cdot \mathbf{r}} \tag{8.46}$$

$$A_j(\mathbf{r}, \omega_j) = |A_j(\mathbf{r}, \omega_j)| e^{j\phi_j} \tag{8.47}$$

or simply

$$\begin{aligned} E_j &= E_j(\mathbf{r}, \omega_j) \\ A_j &= A_j(\mathbf{r}, \omega_j) \end{aligned} \tag{8.48}$$

For instance, it is well known that if two signals with frequencies ω_1 and ω_2 are put into a nonlinear element, the output contains both the upper beat frequency $\omega_1 + \omega_2$ and the lower beat frequency $\omega_1 - \omega_2$. If the analytic signal method is used for this case,

$$\text{Re } (e^{j\omega_1 t} + e^{j\omega_2 t})^2 = \cos 2\omega_1 t + \cos 2\omega_2 t + \cos(\omega_1 + \omega_2)t$$

the lower beat frequency component is missing. A more detailed explanation can be found in Appendix B of Volume 1.

Similarly, the induced electric polarization is expressed as

$$\mathbf{P}_{\mathrm{NL}}(\mathbf{r}, t) = 1/2 \sum_{j=1}^{4} \hat{\mathbf{b}}_j [P_{\mathrm{NL}_j}(\mathbf{r}, \omega_j) e^{-j\omega_j t} + \text{c.c.}] \tag{8.49}$$

$$P_{\mathrm{NL}_j}(\mathbf{r}, \omega_j) = B_j(\mathbf{r}, \omega_j) e^{j\mathbf{k}_j \cdot \mathbf{r}} \tag{8.50}$$

or simply

$$P_{\mathrm{NL}_j} = P_{\mathrm{NL}_j}(\mathbf{r}, \omega_j) \tag{8.51}$$

Next, the actual values of $\mathbf{P}_{\mathrm{NL}}$ will be calculated for a Kerr medium whose susceptibility is predominantly the third order $\chi^{(3)}$.

$$\mathbf{P}_{\mathrm{NL}} = \epsilon_0 \boldsymbol{\chi}^{(3)} \vdots \mathbf{EEE} \tag{8.52}$$

We assume that all $\mathbf{E}$'s are nothing but the waves polarized in the x direction. $\mathbf{E}$, however, consists of waves of four different frequencies, $\omega_1, \omega_2, \omega_3$, and ω_4. All four frequencies are assumed to be in the same frequency range, say, in the visible or infrared region. Their propagation directions and wavelengths are specified by the complex propagation constants $\mathbf{k}_1, \mathbf{k}_2, \mathbf{k}_3$, and $\mathbf{k}_4$.

Inserting Eq. (8.45) into (8.52) gives

$$\begin{aligned} \mathbf{P}_{\mathrm{NL}} = \frac{\hat{\mathbf{x}} \epsilon_0 \chi_{xxxx}}{8} (&E_1 e^{-j\omega_1 t} + E_1^* e^{j\omega_1 t} + E_2 e^{-j\omega_2 t} + E_2^* e^{j\omega_2 t} \\ &+ E_3 e^{-j\omega_3 t} + E_3^* e^{j\omega_3 t} + E_4 e^{-j\omega_4 t} + E_4^* e^{j\omega_4 t})^3 \end{aligned} \tag{8.53}$$

As far as the subscript of χ_{xxxx} is concerned, the first subscript indicates the direction of polarization of the wave emergent from the nonlinear medium and the next three subscripts indicate the directions of polarization of the incident waves. In the present case, all are assumed in the $\hat{\mathbf{x}}$ direction. Manipulation of the cubic in Eq. (8.53) no doubt generates many beat frequencies. The manipulation is shown in Appendix C. We assume that frequencies associated with the third power, such as $3\omega_1, 3\omega_2, \omega_1 + \omega_2 + \omega_4$, and $2\omega_2 + \omega_1$, are all out of the range of interest and are discarded, but all other terms are kept. Terms with frequencies such as $\omega_1 + \omega_2 - \omega_3, \omega_1 + \omega_2 - \omega_4$ or $2\omega_2 - \omega_3$ are of particular interest because they are all in the visible and infrared region.

In order that a significant exchange of energy take place among the frequency components, the generated beat frequency components have to be recycled to participate over and over again in the beating process. For instance, the beating among ω_2, ω_3 and ω_4 creates the original frequency ω_1 if the condition

$$\omega_1 = \omega_3 + \omega_4 - \omega_2 \tag{8.54}$$

is satisfied. This ω_1 frequency component again participates in the beating and creates component ω_2 in accordance with Eq. (8.54), that is, $\omega_2 = \omega_3 + \omega_4 - \omega_1$. These cyclic conversions among the four frequencies are essential for four-wave mixing. If Eq. (8.54) is satisfied, the four frequencies are said to be commensurate. Among the terms in

Appendix C of Volume 1, the following is the set of equations that are commensurate with each other [18].

$$\mathbf{P}_{\mathrm{NL}} = \tfrac{1}{2}\hat{\mathbf{x}}[P_{\mathrm{NL}}(\omega_1)e^{-j\omega_1 t} + P_{\mathrm{NL}}(\omega_2)e^{-j\omega_2 t} + P_{\mathrm{NL}}(\omega_3)e^{-j\omega_3 t} + P_{\mathrm{NL}}(\omega_4)e^{-j\omega_4 t} + \text{c.c.}] \tag{8.55}$$

$$P_{\mathrm{NL}}(\omega_1) = \chi_{\mathrm{eff}}(Q_1 E_1 + 2E_3 E_4 E_2^*) \tag{8.56}$$

$$P_{\mathrm{NL}}(\omega_2) = \chi_{\mathrm{eff}}(Q_2 E_2 + 2E_3 E_4 E_1^*) \tag{8.57}$$

$$P_{\mathrm{NL}}(\omega_3) = \chi_{\mathrm{eff}}(Q_3 E_3 + 2E_1 E_2 E_4^*) \tag{8.58}$$

$$P_{\mathrm{NL}}(\omega_4) = \chi_{\mathrm{eff}}(Q_4 E_4 + 2E_1 E_2 E_3^*) \tag{8.59}$$

where

$$Q_1 = Q - |E_1|^2 \tag{8.60}$$

$$Q_2 = Q - |E_2|^2 \tag{8.61}$$

$$Q_3 = Q - |E_3|^2 \tag{8.62}$$

$$Q_4 = Q - |E_4|^2 \tag{8.63}$$

$$Q = 2(|E_1|^2 + |E_2|^2 + |E_3|^2 + |E_4|^2) \tag{8.64}$$

$$\chi_{\mathrm{eff}} = \frac{3\epsilon_0}{4}\chi_{xxxx} \tag{8.65}$$

Four frequency components are separately associated with the nonlinear wave equation, Eq. (8.39). $P_{\mathrm{NL}}(\omega_1)$ is the source of excitation of E_1, and $P_{\mathrm{NL}}(\omega_2)$ is the source of excitation of E_2, and so on. From Eq. (8.39) and Eqs. (8.56)–(8.59), the following simultaneous differential equations are generated:

$$(\nabla^2 + k_1^2)E_1 = -\mu_0\omega_1^2\chi_{\mathrm{eff}}(Q_1 E_1 + 2E_3 E_4 E_2^*) \tag{8.66}$$

$$(\nabla^2 + k_2^2)E_2 = -\mu_0\omega_2^2\chi_{\mathrm{eff}}(Q_2 E_2 + 2E_3 E_4 E_1^*) \tag{8.67}$$

$$(\nabla^2 + k_3^2)E_3 = -\mu_0\omega_3^2\chi_{\mathrm{eff}}(Q_3 E_3 + 2E_1 E_2 E_4^*) \tag{8.68}$$

$$(\nabla^2 + k_4^2)E_4 = -\mu_0\omega_4^2\chi_{\mathrm{eff}}(Q_4 E_4 + 2E_1 E_2 E_3^*) \tag{8.69}$$

Equations (8.66)–(8.69) are called the coupled wave equations. It should be noted that it is the condition of Eq. (8.54) that allows $E_3E_4E_2^*$ to participate in the generation of E_1. Inserting Eq. (8.46) into Eqs. (8.66)–(8.69), the required vector propagation constants are found. For instance, with Eq. (8.66), the induced polarization (2nd term) has a vector propagation constant of $\mathbf{k}_3 + \mathbf{k}_4 - \mathbf{k}_2$ and the excited E_1 field (1st term) has the propagation constant $\mathbf{k}_1$. An important condition for the maximum transfer of energy of the induced polarization $\mathbf{P}_{\mathrm{NL}}$ into the electric field $\mathbf{E}_1$ is that both waves propagate in phase throughout their paths. The condition of maximum coupling, therefore, is

$$\mathbf{k}_1 = \mathbf{k}_3 + \mathbf{k}_4 - \mathbf{k}_2 \tag{8.70}$$

Similarly, the maximum transfer of energy with Eq. (8.67) is $\mathbf{k}_2 = \mathbf{k}_3 + \mathbf{k}_4 - \mathbf{k}_1$. This equation is exactly identical to Eq. (8.70). Similar conditions generated by Eqs. (8.68) and (8.69) also satisfy Eq. (8.70).

In addition to the previously mentioned frequency condition, Eq. (8.54), the phase matching condition, Eq. (8.70), has to be satisfied simultaneously for the maximum energy coupling.*

In summary, the coupled wave equations govern the exchange of energy among the four different frequency components. In the next section, solutions will be found with an approximation imposed on the coupled wave equation.

8.10.4 Solutions with Bohr's Approximation

Assumptions and approximations are imposed on the coupled wave equations, Eqs. (8.66)–(8.69), to find the differential equations for the amplitudes. The first assumption is that all waves are propagating in the z direction and

$$E_j = \mathbf{A}_j(z)e^{js_jk_jz} \tag{8.71}$$

with $k_j = \omega_j\sqrt{\mu_0\epsilon_0\epsilon_r}$, where $s_j = +1$ when the jth wave propagates in the positive z direction, and $s_j = -1$ when the jth wave propagates in the negative z direction. Inserting Eq. (8.71) into the left hand side of Eq. (8.39) gives

$$(\nabla^2 + k_j^2)E_j = \left(j2s_jk_j\frac{dA_j}{dz} + \frac{d^2A_j}{dz^2}\right)e^{js_jk_jz} \tag{8.72}$$

The second assumption is that the variation of $A_j(z)$ with respect to z is so slow that its second derivative can be ignored compared to other terms. This approximation is called Bohr's approximation or the slowly varying envelope approximation. With these approximations, Eq. (8.39) finally becomes

$$\frac{dA_j}{dz} = js_j\frac{\omega_j}{2}\sqrt{\frac{\mu_0}{\epsilon_0\epsilon_r}}P_{\mathrm{NL}}(\omega_j)e^{-js_jk_jz} \tag{8.73}$$

Insertion of Eqs. (8.56)–(8.59) into Eq. (8.73) results in the following set of equations:

$$\frac{dA_1}{dz} = js_1K_1(Q_1A_1 + 2A_3A_4A_2^*e^{j(s_3k_3+s_4k_4-s_2k_2-s_1k_1)z}) \tag{8.74}$$

$$\frac{dA_2}{dz} = js_2K_2(Q_2A_2 + 2A_3A_4A_1^*e^{j(s_3k_3+s_4k_4-s_1k_1-s_2k_2)z}) \tag{8.75}$$

* In quantum mechanics, the four-photon collision has to satisfy both the conservation of energy,

$$\hbar\omega_1 = \hbar\omega_3 + \hbar\omega_4 - \hbar\omega_2$$

and the conservation of momentum

$$\hbar\mathbf{k}_1 = \hbar\mathbf{k}_3 + \hbar\mathbf{k}_4 - \hbar\mathbf{k}_2$$

where $\hbar = h/2\pi$ and h is Planck's constant.

$$\frac{dA_3}{dz} = js_3K_3(Q_3A_3 + 2A_1A_2A_4^* e^{j(s_1k_1+s_2k_2-s_4k_4-s_3k_3)z}) \tag{8.76}$$

$$\frac{dA_4}{dz} = js_4K_4(Q_4A_4 + 2A_1A_2A_3^* e^{j(s_1k_1+s_2k_2-s_3k_3-s_4k_4)z}) \tag{8.77}$$

$$K_j = \frac{\omega_j}{2}\sqrt{\frac{\mu_0}{\epsilon_0\epsilon_r}}\chi_{\text{eff}} \tag{8.78}$$

Example 8.1 Figure 8.16 shows an arrangement for generating a phase conjugate wave using the principle of holography [20]. Explain the operation using the coupled wave equations.

Solution All frequencies used in the hologram are the same and

$$\omega_1 = \omega_2 = \omega_3 = \omega_4 = \omega \tag{8.79}$$

This satisfies the frequency condition in Eq. (8.54). Let E_3 and E_4 be the signal wave E_s and phase conjugate wave E_c, respectively. Let the propagation directions of these two waves be along the z axis as shown in Fig. 8.16, with $s_3 = +1$ for E_3 and $s_4 = -1$ for E_4.

$$\begin{aligned} E_3 &= E_s = A_s e^{jk_s z} \\ E_4 &= E_c = A_c e^{-jk_c z} \end{aligned} \tag{8.80}$$

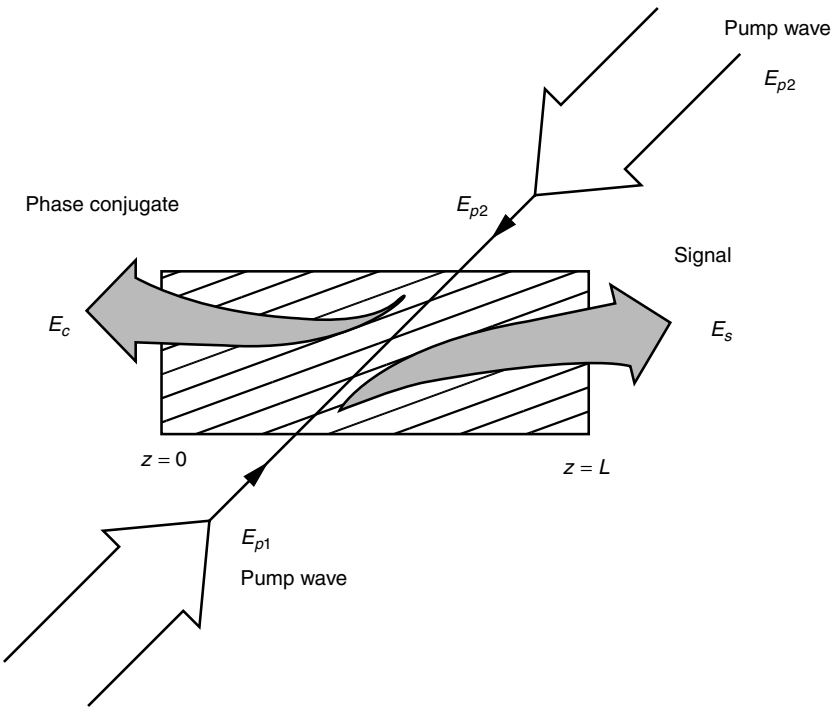

Figure 8.16 Generating a phase conjugate wave from a hologram.

Let the two pump waves E_{p_1} and E_{p_2} be represented by

$$\begin{aligned} E_1 &= E_{p_1} = A_p e^{j\mathbf{k}_{p_1}\cdot\mathbf{r}} \\ E_2 &= E_{p_2} = A_p e^{j\mathbf{k}_{p_2}\cdot\mathbf{r}} \end{aligned} \tag{8.81}$$

Their amplitudes are assumed equal. Furthermore, the amplitudes of the pump waves are assumed to be so large that the depletion of the energy into either the signal or phase conjugate waves is negligible, and the amplitudes can be considered not only constant with respect to distance but also

$$\begin{aligned} |A_p|^2 &>> |A_s|^2 \\ |A_p|^2 &>> |A_c|^2 \end{aligned} \tag{8.82}$$

The signal and conjugate waves propagate in opposite directions, so that

$$\mathbf{k}_3 + \mathbf{k}_4 = 0 \tag{8.83}$$

and

$$\begin{aligned} s_3 &= +1 \\ s_4 &= -1 \end{aligned} \tag{8.84}$$

and in order to satisfy Eq. (8.70),

$$\mathbf{k}_{p_1} + \mathbf{k}_{p_2} = 0 \tag{8.85}$$

With Eq. (8.80)–(8.85), the coupled wave equations, Eqs. (8.76) and (8.77), become

$$\begin{aligned} \frac{dA_s}{dz} &= jK\{2|A_p|^2 A_s + A_p^2 A_c^*\} \\ \frac{dA_c}{dz} &= -jK\{2|A_p|^2 A_c + A_p^2 A_s^*\} \end{aligned} \tag{8.86}$$

where

$$K = \omega\sqrt{\frac{\mu_0}{\epsilon_0\epsilon_r}}\chi_{\text{eff}} \tag{8.87}$$

In order to remove the first term from the right-hand side of Eq. (8.86), the amplitude and phase factors of A_s and A_c are explicitly written as

$$\begin{aligned} A_s &= A_{s0}e^{+j\beta_{\text{NL}}z} \\ A_c &= A_{c0}e^{-j\beta_{\text{NL}}z} \\ A_{s0} &= A_{s0}(z) \\ A_{c0} &= A_{c0}(z) \end{aligned} \tag{8.88}$$

where

$$\beta_{\mathrm{NL}} = 2K|A_p|^2 \tag{8.89}$$

Inserting Eq. (8.88) into (8.86) gives

$$\frac{dA_{s0}}{dz} = jKA_p^2 A_{c0}^* \tag{8.90}$$

$$\frac{dA_{c0}}{dz} = -jKA_p^2 A_{s0}^* \tag{8.91}$$

Taking the derivative of Eq. (8.90) and inserting Eq. (8.91) gives

$$\frac{d^2A_{c0}}{dz^2} + K^2|A_p|^4 A_{c0} = 0 \tag{8.92}$$

and similarly,

$$\frac{d^2A_{s0}}{dz^2} + K^2|A_p|^4 A_{s0} = 0 \tag{8.93}$$

The general solution of Eq. (8.92) is

$$A_{c0} = A\cos K|A_p|^2 z + B\sin K|A_p|^2 z \tag{8.94}$$

From Eqs. (8.91) and (8.94), A_{s0}^* is expressed as

$$A_{s0}^* = j\frac{A_p^*}{A_p}(-A\sin K|A_p|^2 z + B\cos K|A_p|^2 z) \tag{8.95}$$

The integration constants A and B are determined from the boundary conditions:

$$A_{c0}(L) = 0 \quad \text{at } z = L \tag{8.96}$$

$$A_s(0) = A_{s0}(0) \quad \text{at } z = 0 \tag{8.97}$$

From Eqs. (8.94) and (8.96), the integration constant A is

$$A = -B\tan K|A_p|^2 L \tag{8.98}$$

From Eqs. (8.95) and (8.97), the integration constant B is

$$B = \frac{A_p}{jA_p^*}A_{s0}^*(0) \tag{8.99}$$

Inserting these constants into Eq. (8.94) and using Eq. (8.88) gives

$$A_c(z) = j\frac{A_p}{A_p^*}A_s^*(0)e^{-j\beta_{\mathrm{NL}}z}\frac{\sin K|A_p|^2(L-z)}{\cos K|A_p|^2 L} \tag{8.100}$$

and similarly, inserting Eqs. (8.98) and (8.99) into Eq. (8.95) and using Eq. (8.88) gives

$$A_s(z) = A_s(0)e^{j\beta_{\mathrm{NL}}z}\frac{\cos K|A_p|^2(L-z)}{\cos K|A_p|^2L} \tag{8.101}$$

Now let us interpret the calculated results. From Eq. (8.100), the magnitude of $A_c(z)$ increases with distance from the back surface at $z = L$. Referring to Fig. 8.16, the pump wave E_{p_2} is depleted into the phase conjugate wave by the deflection from the fringes established by E_{p_1} and E_s and is accumulated toward the front surface at $z = 0$. Similarly, the signal wave $A_s(z)$ grows from the front surface to the back surface $z = L$ by the depletion of the pump wave E_{p_1} into E_s. □

8.11 THE GAIN OF FORWARD FOUR-WAVE MIXING

The geometry shown in Fig. 8.16 is one example that satisfies both the frequency and phase matching conditions. In this geometry, not only the two pump waves are counterpropagating but also the signal and phase conjugate waves are counterpropagating. In order to meet the phase matching condition of Eq. (8.70), each side of

$$\mathbf{k}_1 + \mathbf{k}_2 = \mathbf{k}_3 + \mathbf{k}_4 \tag{8.102}$$

was set individually to zero. The frequency condition, Eq. (8.54),

$$\omega_1 + \omega_2 = \omega_3 + \omega_4 \tag{8.103}$$

was met by letting all the frequencies be the same.

Another geometry will be investigated here. This time, all the waves are copropagating in the forward direction [16,21]. It is certainly possible to meet the condition of Eq. (8.102) by choosing identical **k**'s and choosing identical frequencies to meet the condition of Eq. (8.103). In the earlier counterpropagating case, a half-mirror was good enough to separate the phase conjugate and signal waves. This is not possible in the copropagating case. A remedy for this is the use of multiple frequencies that meet the frequency condition of Eq. (8.103). One way this can be done is to set the average value of ω_3 and ω_4 equal to the average value of ω_1 and ω_2, as shown in Fig. 8.17a.

A special case of Fig. 8.17a is shown in Fig. 8.17b. That special case occurs when ω_1 and ω_2 are identical, and the four-wave mixing is semidegenerate. This arrangement, when ω_1 (or ω_2) is taken as a pump wave, necessitates only one pump wave and simplifies the implementation. Figure 8.18 shows the implementation. The signal and pump waves are fed into a dispersion-shifted fiber and the outputs are the phase conjugate, signal, and pump waves, among which the phase conjugate wave is selected by means of an optical filter. The core glass of the dispersion-shifted fiber is used as the $\chi^{(3)}$ nonlinear medium.

Next, the output powers of the signal and phase conjugate waves are calculated using the coupled wave equations, Eqs. (8.74)–(8.77). The procedure is quite similar to

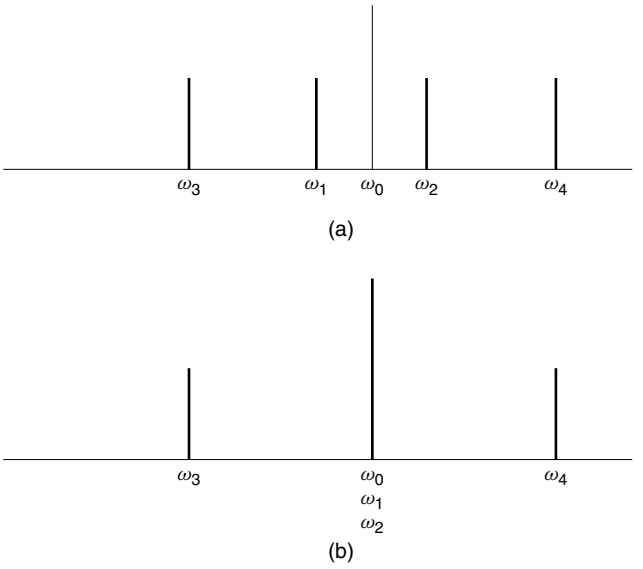

Figure 8.17 Spectra of forward four-wave mixing. (a) Nondegenerate case. (b) Semidegenerate case.

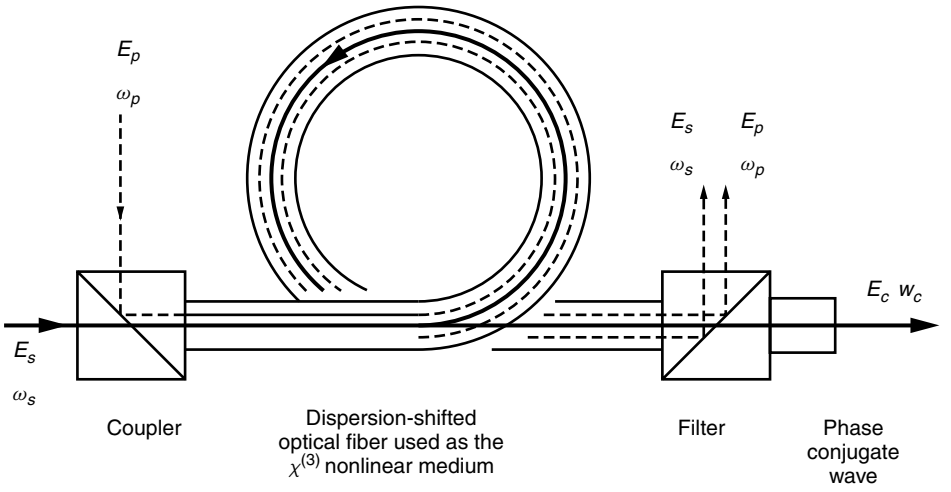

Figure 8.18 Forward four-wave mixing.

the reflection type presented in Example 8.1, and emphasis is placed on pointing out the differences, as well as the significance of the phase matching condition imposed on $\mathbf{k}_j$ by Eq. (8.70). Referring to Fig. 8.18, let us denote

$$E_1 = E_2 = A_p e^{jk_p z} \tag{8.104}$$

$$E_3 = E_s = A_s e^{jk_s z} \tag{8.105}$$

$$E_4 = E_{\text{pc}} = A_c e^{jk_c z} \tag{8.106}$$

In this case, all waves are propagating in the forward direction, and

$$s_j = 1 \tag{8.107}$$

With Eq. (8.82), the coupled wave equations, Eqs. (8.74)–(8.77), become

$$\frac{dA_p}{dz} \approx j\tfrac{3}{2}K|A_p|^2A_p \tag{8.108}$$

$$\frac{dA_s}{dz} = jK(2|A_p|^2A_s + A_p^2A_c^*e^{j\Delta kz}) \tag{8.109}$$

$$\frac{dA_c}{dz} = jK(2|A_p|^2A_c + A_p^2A_s^*e^{j\Delta kz}) \tag{8.110}$$

$$\Delta k = k_1 + k_2 - k_3 - k_4 \tag{8.111}$$

In order to remove the first terms from both Eqs. (8.109) and (8.110), the amplitude and phase factors of A_s and A_c are explicitly written as

$$A_s = A_{s0}e^{j\beta_{\mathrm{NL}}z} \tag{8.112}$$

$$A_c = A_{c0}e^{j\beta_{\mathrm{NL}}z} \tag{8.113}$$

$$\beta_{\mathrm{NL}} = 2k|A_p|^2$$

Inserting the expressions for A_s and A_c in Eqs. (8.112) and (8.113) into Eqs. (8.109) and (8.110) gives

$$\frac{dA_{s0}}{dz} = jKA_p^2A_{c0}^*e^{j(\Delta k-2\beta_{\mathrm{NL}})z} \tag{8.114}$$

$$\frac{dA_{c0}}{dz} = jKA_p^2A_{s0}^*e^{j(\Delta k-2\beta_{\mathrm{NL}})z} \tag{8.115}$$

The procedure for solving the differential equations starts with Eq. (8.108). The solution of Eq. (8.108) with the boundary condition $A_p = A_p(0)$ at $z = 0$ is

$$A_p = A_p(0)e^{j\beta_p z} \tag{8.116}$$

where

$$\beta_p = \tfrac{3}{2}K|A_p|^2 \tag{8.117}$$

It should be noted that both β_p and β_{NL} are a function of the intensity $|A_p|^2$ and are nonlinear with the pump field.

Inserting Eq. (8.116) into Eqs. (8.114) and (8.115) gives

$$\frac{dA_{s0}}{dz} = jKA_p^2(0)A_{c0}^*e^{j\Gamma z} \tag{8.118}$$

$$\frac{dA_{c0}^*}{dz} = -jKA_p^2(0)A_{s0}e^{-j\Gamma z} \tag{8.119}$$

where

$$\Gamma = 2(\beta_p - \beta_{NL}) + \Delta k \tag{8.120}$$

With Eqs. (8.89) and (8.117), Eq. (8.120) is further rewritten as

$$\Gamma = \Delta k - KA_p^2(0) \tag{8.121}$$

Assumed solutions

$$A_{s0} = [Ae^{gz} + Be^{-gz}]e^{j(\Gamma/2)z} \tag{8.122}$$

$$A_{c0}^* = [Ce^{gz} + De^{-gz}]e^{-j(\Gamma/2)z} \tag{8.123}$$

are put into Eqs. (8.118) and (8.119). The prime target of this calculation is to obtain the value of the gain g.

Let

$$KA_p^2(0) = a \tag{8.124}$$

Inserting Eqs. (8.122) and (8.123) into Eq. (8.118) gives

$$[(g + j\Gamma/2)A - jaC]e^{(g+j\Gamma/2)z} + [(-g + j\Gamma/2)B - jaD]e^{(-g+j\Gamma/2)z} = 0 \tag{8.125}$$

For Eq. (8.125) to be satisfied for any value of z, the values in the square brackets have to vanish:

$$(g + j\Gamma/2)A - jaC = 0 \tag{8.126}$$

$$(-g + j\Gamma/2)B - jaD = 0 \tag{8.127}$$

Similarly, inserting Eqs. (8.122) and (8.123) into Eq. (8.119) gives

$$jaA + (g - j\Gamma/2)C = 0 \tag{8.128}$$

$$jaB - (g + j\Gamma/2)D = 0 \tag{8.129}$$

Equations (8.126)–(8.129) are rearranged in a matrix form as

$$\begin{vmatrix} (g + j\Gamma/2) & 0 & -ja & 0 \\ 0 & (-g + j\Gamma/2) & 0 & -ja \\ ja & 0 & (g - j\Gamma/2) & 0 \\ 0 & ja & 0 & -(g + j\Gamma/2) \end{vmatrix} \begin{vmatrix} A \\ B \\ C \\ D \end{vmatrix} = 0 \tag{8.130}$$

For nonzero A, B, C, and D to exist, the determinant of Eq. (8.130) has to vanish. The value of the determinant is

$$[g^2 + (\Gamma/2)^2 - a^2]^2 = 0 \tag{8.131}$$

and finally,

$$g = \pm\sqrt{a^2 - (\Gamma/2)^2} \tag{8.132}$$

Putting back the parameters from Eqs. (8.121) and (8.124) gives

$$g = \sqrt{(2KA_p^2(0))^2 - (\Delta k - KA_p^2(0))^2}/2 \tag{8.133}$$

Thus, for a given value of A_p, the gain g becomes maximum when

$$\Delta k - KA_p^2(0) = 0$$

That is, when the combination of the linear and nonlinear phase factors becomes zero rather than Δk alone becomes zero.

If $A_{c0} = 0$, at $z = 0$, from Eq. (8.123),

$$C = -D \tag{8.134}$$

and with Eqs. (8.113) and (8.134), Eq. (8.123) becomes

$$A_c(z) = 2C \sinh(gz) e^{j(\beta_{\mathrm{NL}} + \Gamma/2)z} \tag{8.135}$$

The amplitude of the conjugate wave increases with the hyperbolic sine of the distance.

8.12 PULSE BROADENING COMPENSATION BY FORWARD FOUR-WAVE MIXING

Pulse broadening in an optical fiber limits the transmission capability of fiber optic communication. A method for narrowing a broadened light pulse is by means of four-wave mixing [13,22–24]. The principle is exactly the same as that illustrated in Fig. 8.5, where the distorted wave is reflected by a phase conjugator and retraces the time history of the distortion up to the original waveform as it goes back through the distorting medium again.

When applying this principle to fiber optic communication systems, a phase conjugator is placed in the middle of the transmission cable. The signal wave propagates down the first half of the fiber cable, and the phase conjugate wave is funneled into the second half of the fiber cable. An assumption has to be made that both halves of the fiber have the same physical properties and the same length.

Figure 8.19 shows the scheme for pulse broadening compensation by means of semidegenerate forward four-wave mixing with $\omega_1 = \omega_2 = \omega_p$, $\omega_3 = \omega_s$ and $\omega_4 = \omega_c$. Referring to Fig. 8.19, the transmitter light pulse is fed into a single mode optical fiber of length L_1. At L_1, the pulse enters the phase conjugator. The phase conjugator utilizes the nonlinear property of the core glass of a dispersion-shifted fiber. The broadband nature of the dispersion-shifted fiber allows for easy phase matching among the signal, phase conjugate, and pump waves. The pump wave is added to the signal by means of a beam combiner to drive the phase conjugator. Both the pump and the signal waves are removed at the exit of the phase conjugator by means of an optical filter. Only the phase conjugate wave is fed into the other half of the single mode fiber. The phase conjugate wave travels a distance L_2 to the receiver. If $L_1 = L_2$, then the transmitted pulse will be recovered when the phase conjugate wave reaches the receiver.

Now let us analyze the compensation process in more detail. Referring again to Fig. 8.19, a light pulse $E_1(z, t)$ is launched into a single mode fiber at $z = 0$. The

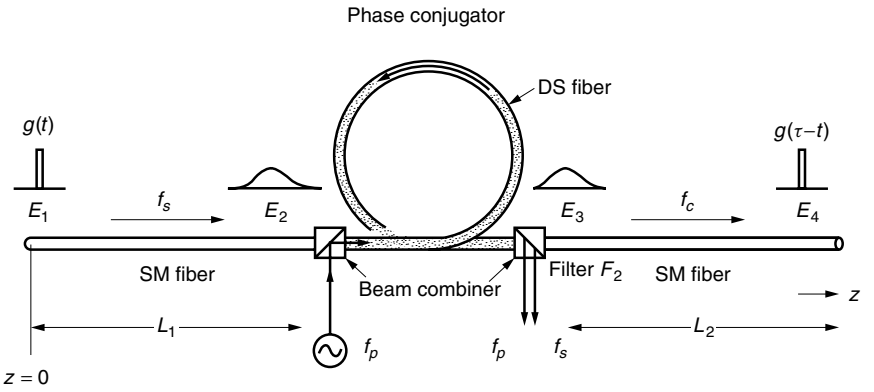

Figure 8.19 Pulse broadening compensation by four-wave mixing. DS fiber, dispersion-shifted fiber; SM fiber, single mode fiber.

carrier frequency f_s of the light pulse is modulated by an envelope function $g(t)$:

$$E_1(0, t) = g(t) \cos 2\pi f_s t \tag{8.136}$$

The frequency spectra of the input light is obtained by the Fourier transform as

$$\mathcal{F}(E_1) = \tfrac{1}{2}[G(f - f_s) + G(f + f_s)] \tag{8.137}$$

where

$$\mathcal{F}\{g(t)\} = G(f) \tag{8.138}$$

The Fourier transform $G(f)$ of the envelope is shifted by f_s to the right and by $-f_s$ to the left in the frequency domain. The narrower the width of the input pulse in time, the greater the spread of the spectra in the frequency domain.

Each frequency component in this spectra propagates at its own phase velocity and reaches the receiver. Unless each frequency component propagates at the same velocity, the relative phase relationship is upset and the received pulse becomes distorted.

First, the behavior of a single frequency wave as it propagates to its destination is analyzed. Once the behavior of one frequency component is known, the received pulse shape is obtained by integrating over frequency.

Let the chosen frequency be $f = f_s + \eta$, which is η away from f_s. From Eq. (8.137), this frequency component has an amplitude of $\frac{1}{2}G(\eta)$. The propagation of this frequency component through the first half L_1 of a long fiber is

$$dE_2 = \tfrac{1}{2}G(\eta)\, d\eta e^{-j2\pi(f_s+\eta)t + j\beta(f_s+\eta)L_1} + \text{c.c.} \tag{8.139}$$

The value of the propagation constant β at $f_s + \eta$ can be approximated by the Taylor series expansion, η being usually at most one thousandth of f_s,

$$\beta(f_s + \eta) = \beta(f_s) + \beta'(f_s)\eta + \tfrac{1}{2}\beta''(f_s)\eta^2 + \cdots \tag{8.140}$$

Thus, the expression for the single frequency spectrum at the input to the phase conjugator is

$$dE_2 = \tfrac{1}{2}G(\eta)\, d\eta e^{-j2\pi(f_s+\eta)t} e^{+j\beta(f_s)L_1 + j\beta'(f_s)L_1\eta + \frac{1}{2}j\beta''(f_s)L_1\eta^2} + \text{c.c.} \tag{8.141}$$

The output dE_3 from the phase conjugator is the phase conjugate of the input except for the time factor,

$$dE_3(\eta) = \tfrac{1}{2}\sqrt{\eta_c}G^*(\eta)\,d\eta e^{-j2\pi(f_s+\eta)t}e^{-j\beta(f_s)L_1-j\beta'(f_s)L_1\eta-\frac{1}{2}j\beta''(f_s)L_1\eta^2} + \text{c.c.} \tag{8.142}$$

where η_c is the conversion efficiency, which is determined by such parameters as the gain given by Eq. (8.133), fiber loss and beam combiner loss.

In the second half of the optical fiber, the phase conjugate wave propagates. In the degenerate case of Eq. (8.103), the frequency f_c of the phase conjugate wave is shifted to the other side of the pump frequency f_p, as shown in Fig. 8.17b, and

$$f_c = 2f_p - f_s \tag{8.143}$$

With the input of $f_s + \eta$, the new shifted frequency f_c' is

$$f_c' = f_c - \eta \tag{8.144}$$

The propagation constant in the second fiber at frequency $f_c - \eta$ is obtained from the Taylor series expansion

$$\beta(f_c - \eta) = \beta(f_c) - \beta'(f_c)\eta + \tfrac{1}{2}\beta''(f_c)\eta^2 + \cdots \tag{8.145}$$

The signal reaching the receiver is therefore

$$\begin{aligned} dE_4(\eta) = {} & \tfrac{1}{2}\sqrt{\eta_c}G^*(\eta)d\eta e^{j[-2\pi(f_c-\eta)t+\beta(f_c)L_2-\beta(f_s)L_1]} \\ & \times e^{-j[\beta'(f_s)L_1+\beta'(f_c)L_2]\eta+\frac{1}{2}j[\beta''(f_c)L_2-\beta''(f_s)L_1]\eta^2} + \text{c.c.} \end{aligned} \tag{8.146}$$

where the f_s and f_p components have been filtered out by filter F_2.

Let us put

$$\phi = \beta(f_c)L_2 - \beta(f_s)L_1 \tag{8.147}$$

$$\tau = \frac{1}{2\pi}[\beta'(f_c)L_2 + \beta'(f_s)L_1] \tag{8.148}$$

$$\psi = \tfrac{1}{2}[\beta''(f_c)L_2 - \beta''(f_s)L_1] \tag{8.149}$$

$$dE_4(\eta) = \tfrac{1}{2}\sqrt{\eta_c}G^*(\eta)\,d\eta e^{-j2\pi f_c t+j\phi+j2\pi(t-\tau)\eta+j\psi\eta^2} + \text{c.c.} \tag{8.150}$$

The waveform of the received signal is obtained by integrating over frequency:

$$E_4 = \tfrac{1}{2}\sqrt{\eta_c}e^{-j2\pi f_c t+j\phi}\int G^*(\eta)e^{j2\pi(t-\tau)\eta+j\psi\eta^2}\,d\eta + \text{c.c.} \tag{8.151}$$

First, let us deal with the case when

$$\psi = 0 \tag{8.152}$$

Equation (8.151) is in the form of an inverse Fourier transform and

$$E_4(L_1 + L_2, t) = \tfrac{1}{2}\sqrt{\eta_c}e^{-j2\pi f_c t + j\phi}g^*(\tau - t) + \text{c.c.} \tag{8.153}$$

If the envelope function g is assumed real, the final result is

$$E_4(L_1 + L_2, t) = \sqrt{\eta_c}g(\tau - t)\cos(-2\pi f_c t + \phi) \tag{8.154}$$

Equation (8.154) shows that the envelope function of the received pulse is exactly the same as that of the transmitted pulse except that $g(\tau - t)$ is time reversed. The original envelope $g(0)$ reappears τ seconds later. Thus, τ is the total transmission time of the envelope from $z = 0$ to $z = L_1 + L_2$.

Next, the case when $\psi \neq 0$ is considered. Equation (8.151) becomes

$$E_4 = e^{-j2\pi f_c t + j\phi}g(\tau - t) * \mathcal{F}^{-1}\{e^{-j\Psi\eta^2}\} \tag{8.155}$$

The pulse shape is now convolved with $\mathcal{F}^{-1}\{e^{-j\psi\eta^2}\}$, creating a distortion in the received pulse. The distortionless condition, however, can be achieved from Eq. (8.149) by setting

$$\beta''(f_c)L_2 = \beta''(f_s)L_1 \tag{8.156}$$

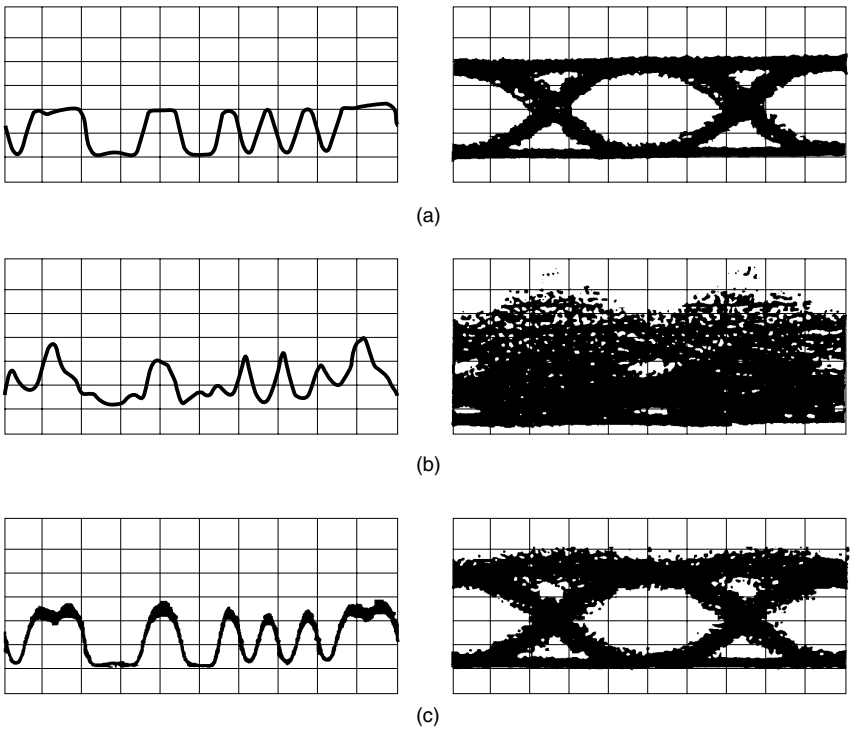

Figure 8.20 Received pulse shapes of (1110001100101010) coded patterns and eye-patterns for a 10-Gb/s intensity modulated signal at $P_1 = P_2 = +5$ dBm. (a) A 5-m transmission without OPC. (b) A 200-km transmission without OPC. (c) A 200-km transmission with OPC at the midpoint. (Scale units of pulse shapes in left column: V, 50 mV/div.; H, 200 ps/div. Scale units of pulse shapes in right column: V, 25 mV/div.; H, 20 ps/div. (After S. Watanabe et al. [22].)

One way of obtaining this condition is to use a fiber with the same length for both halves of the transmission cable.

Pulse broadening compensation with 10 Gb/s pulse modulated light is demonstrated in Fig. 8.20 [22]. Figure 8.20a shows the input signal. Figure 8.20b shows the same signal after 200-km transmission without the optical phase conjugator (OPC) and Fig. 8.20c shows the result when the phase conjugator is inserted in the middle of the fiber transmission. Figure 8.20 confirms the effectiveness of pulse broadening compensation in an optical fiber by means of four-wave mixing.

PROBLEMS

8.1 In the text, the distorting medium in Fig. 8.4 was assumed to be free of temporal variations: that is, the temporal variations either did not exist or were so slow that they could be taken as constant for the duration of the experiment. Consider a distorting medium in which temporal fluctuations cannot be ignored. For simplicity, assume that the fluctuation is sinusoidal with time and is expressed as $\Phi(t) = \Phi \cos \omega t$. What are the distances L between the distorting medium and the phase conjugate mirror (Fig. P8.1) that make the best distortion-free image and the worst distorted image?

8.2 Consider a crystal whose one-dimensional charge distribution is as shown in Fig. P8.2.

(a) Does this crystal have inversion symmetry?

(b) Draw the redistributed charges when exposed to the **E** field of an incident light wave.

(c) Does such a crystal possess a second order nonlinearity?

8.3 Does a crystal with inversion symmetry have a fourth order nonlinearity?

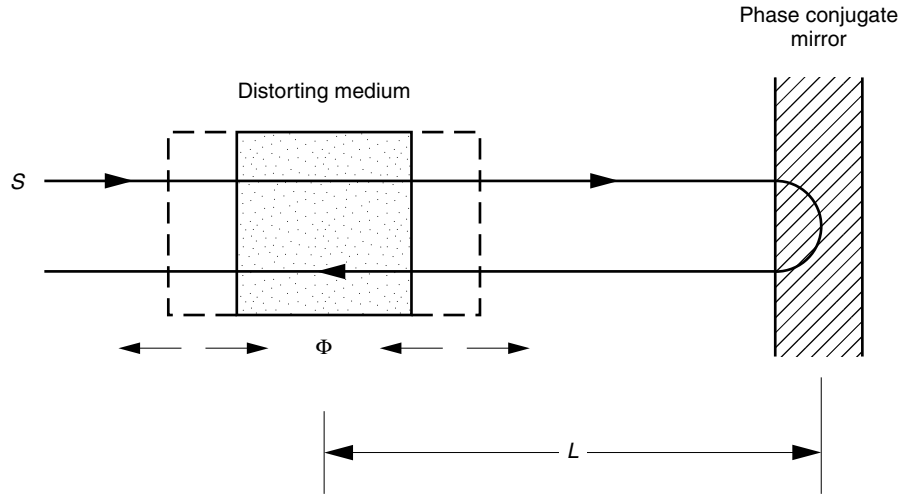

Figure P8.1 Temporally varying distorting medium.

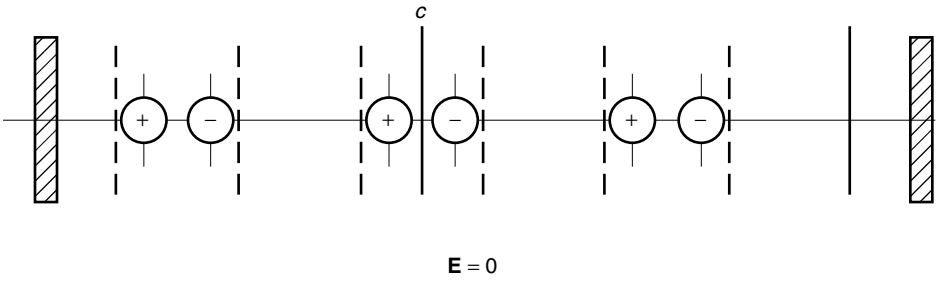

Figure P8.2 Does this crystal have nonzero $\chi^{(2)}$?

8.4 Three lightwaves having adjacent frequencies are incident onto an optical fiber (Fig. P8.4). Find the frequency spectra generated in the fiber due to the third order nonlinear effect. All incident waves are assumed to be polarized in the x direction [25].

8.5 Assuming the degenerate case, if the directions of $\mathbf{k}_1$ and $\mathbf{k}_2$ are set as shown in Fig. P8.5, find the directions of $\mathbf{k}_3$ and $\mathbf{k}_4$ that sustain four-wave mixing.

8.6 Draw all possible fringe patterns in a medium when four waves are incident as shown in Fig. P8.6.

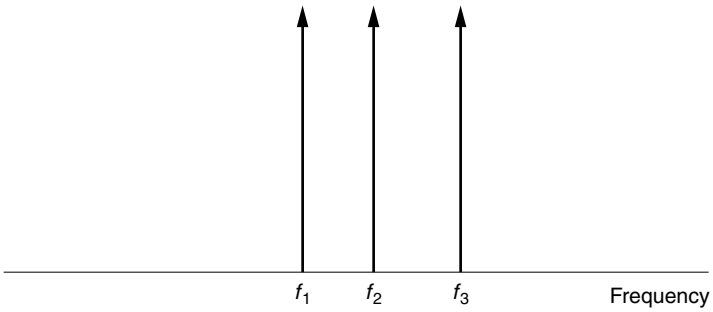

Figure P8.4 Spectra of light incident onto an optical fiber having a third order nonlinearity.

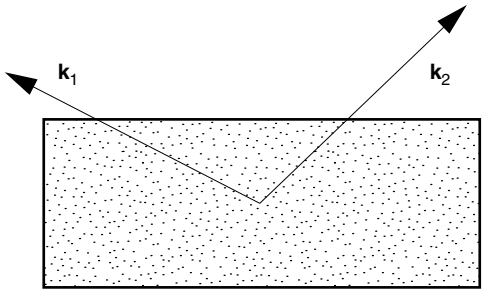

Figure P8.5 Finding the condition of four-wave mixing.

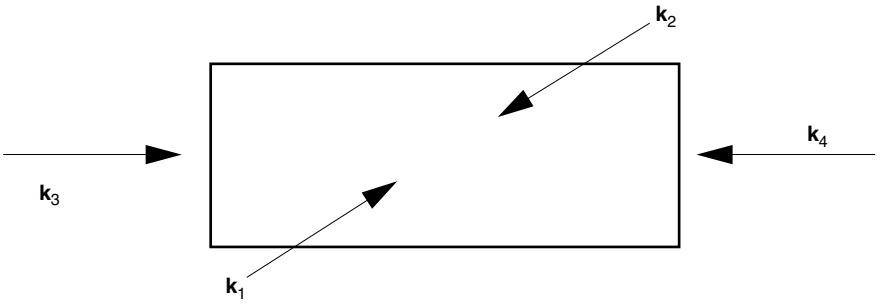

Figure P8.6 A configuration for a degenerate type of four-wave mixing.

8.7 In the text, the case of forward four-wave mixing was dealt with, but the attenuation in the dispersion-shifted fiber was not taken into consideration. With an amplitude attenuation constant α, Eqs. (8.108)–(8.111) become

$$\frac{dA_p}{dz} = (-\alpha + j\tfrac{3}{2}K|A_p|^2)A_p$$

$$\frac{dA_s}{dz} = (-\alpha + j2K|A_p|^2)A_s + jKA_p^2A_c^*e^{j\Delta kz}$$

$$\frac{dA_c}{dz} = (-\alpha + j2K|A_p|^2)A_c + jKA_p^2A_s^*e^{j\Delta kz}$$

Find the differential equations with attenuation in the fiber.

REFERENCES

1. D. M. Pepper, "Applications of optical phase conjugation," *Sci. Am.*, 74–83 (Jan. 1986).
2. H. Kogelnik, "Reconstructing response and efficiency of hologram gratings," *Proceedings of the Symposium on Modern Optics*, Polytechnic Press, Brooklyn, NY, 1967, pp. 605–617.
3. D. M. Pepper, "Nonlinear optical phase conjugation," *Opt. Eng.*, **21**(2), 156–183 (1982).
4. R. W. Hellwarth, "Third-order optical susceptibilities of liquids and solids," *Prog. Quantum Electron.*, **5**, 1–68 (1977).
5. J. Feinberg, "Self-pumped, continuous-wave phase conjugator using internal reflection," *Opt. Lett.*, **7**(10), 486–488 (1982).
6. D. M. Bloom and G. C. Bjorklund, "Conjugate wave-front generation and image reconstruction for four-wave mixing," *Appl. Phys. Lett.*, **31**(9), 592–594 (1977).
7. V. V. Shkunov and B. Ya. Zel'dovich, "Optical phase conjugation," *Sci. Am.*, 54–59 (Dec. 1985).
8. B. Fischer, M. Cronin-Golomb, J. O. White, and A. Yariv, "Real-time phase conjugate window for one-way optical field imaging through a distortion," *Appl. Phys. Lett.*, **41**(2), 141–143 (1982).
9. A. Chiou, P. Yeh, C.-X. Yang, and C. Gu, "Experimental demonstration of photorefractive resonator for adaptive fault-tolerant coupling," *Opt. Photonics News*, 20–21 (Dec. 1995).
10. P. Yeh, "Photorefractive phase conjugators," *Proc. IEEE*, **80**(3), 436–450 (1992).

11. M. Cronin-Golomb, B. Fischer, J. O. White, and A. Yariv, "Theory and applications of four-wave mixing in photorefractive media," *IEEE J. Quaautum Electron.*, **QE-20**(4), 12–30 (1984).
12. Y. Owechko, G. J. Dunning, E. Marom, and B. H. Soffer, "Holographic associative memory with nonlinearities in the correlation domain," *Appl. Opt.* **26**(10), 1900–1910 (1987).
13. A. Yariv, *Optical Electronics*, 4th ed., Saunders, New York, 1991.
14. Y. R. Shen, *Principles of Nonlinear Optics*, Wiley, New York, 1984.
15. R. A. Fisher (Ed.), *Optical Phase Conjugation*, Academic Press, New York, 1983.
16. G. P. Agrawal, *Applications of Nonlinear Fiber Optics*, Academic Press, San Diego, CA, 2001.
17. N. Bloembergen, *Nonlinear Optics*, 4th ed., World Scientific, River Edge, NJ, 1996.
18. B. E. A. Saleh and M. C. Teich, *Fundamentals of Photonics*, Wiley, New York, 1991.
19. G. C. Baldwin, *An Introduction to Nonlinear Optics*, Plenum Press, New York, 1974.
20. A. Yariv, D. Fekete, and D. M. Pepper, "Compensation for channel dispersion by nonlinear optical phase conjugation," *Opt. Lett.*, **4**(2), 52–54 (1979).
21. R. H. Stolen and J. E. Bjorkholm, "Parametric amplification and frequency conversion in optical fibers," *IEEE J. Quantum Electron.*, **QE 18**(7), 1062–1072 (1982).
22. S. Watanabe, G. Ishikawa, T. Naito, and T. Chikama, "Generation of optical phase-conjugate waves and compensation for pulse shape distortion in a single-mode fiber," *J. Lightwave Technol.*, **12**(12), 2139–2146 (1994).
23. N. Shibata, R. P. Braun, and R. G. Waarts, "Phase-mismatch dependence of efficiency of wave generation through four-wave mixing in a single-mode optical fiber," *IEEE J. Quantum Electron.*, **QE-23**(7), 1205–1210 (1987).
24. S. Murata, A. Tomita, J. Shimizu, and A. Suzuki, "THz optical-frequency conversion of 1 Gb/s-signals using highly nondegenerate four-wave mixing in an InGaAsP semiconductor laser," *IEEE Photonics Technol. Lett.*, **3**(11), 1021–1023 (1991).
25. M. W. Maeda, W. B. Sessa, W. I. Way, A. Yi-Yan, L. Curtis, R. Spicer, and R. I. Laming, "The effect of four-wave mixing in fibers on optical frequency-division multiplexed systems," *J. Lightwave Technol.*, **8**(9), 1402–1408 (1990).